

**NASA  
Reference  
Publication  
1181**

August 1987

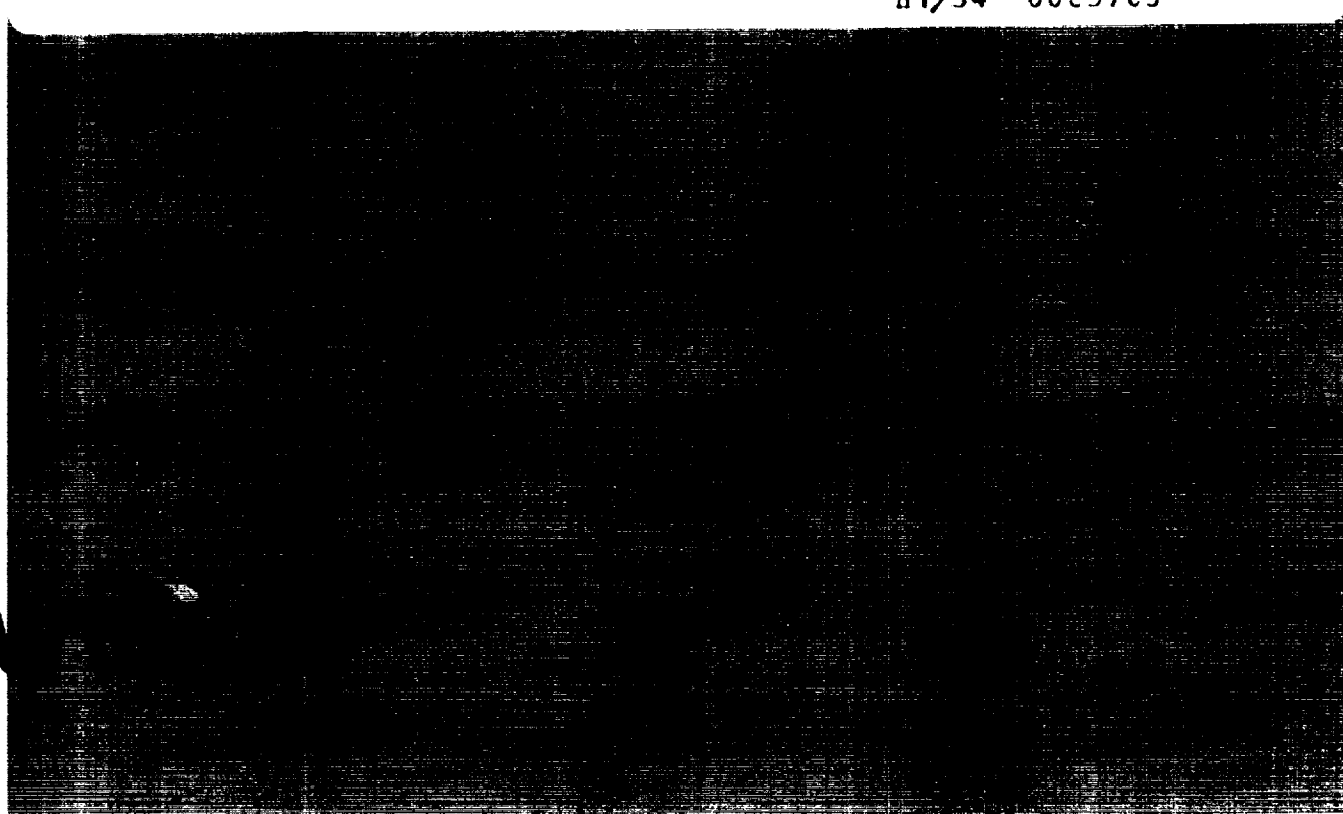
# Simplified Curve Fits for the Thermodynamic Properties of Equilibrium Air

S. Srinivasan,  
J. C. Tannehill,  
and K. J. Weilmuenster

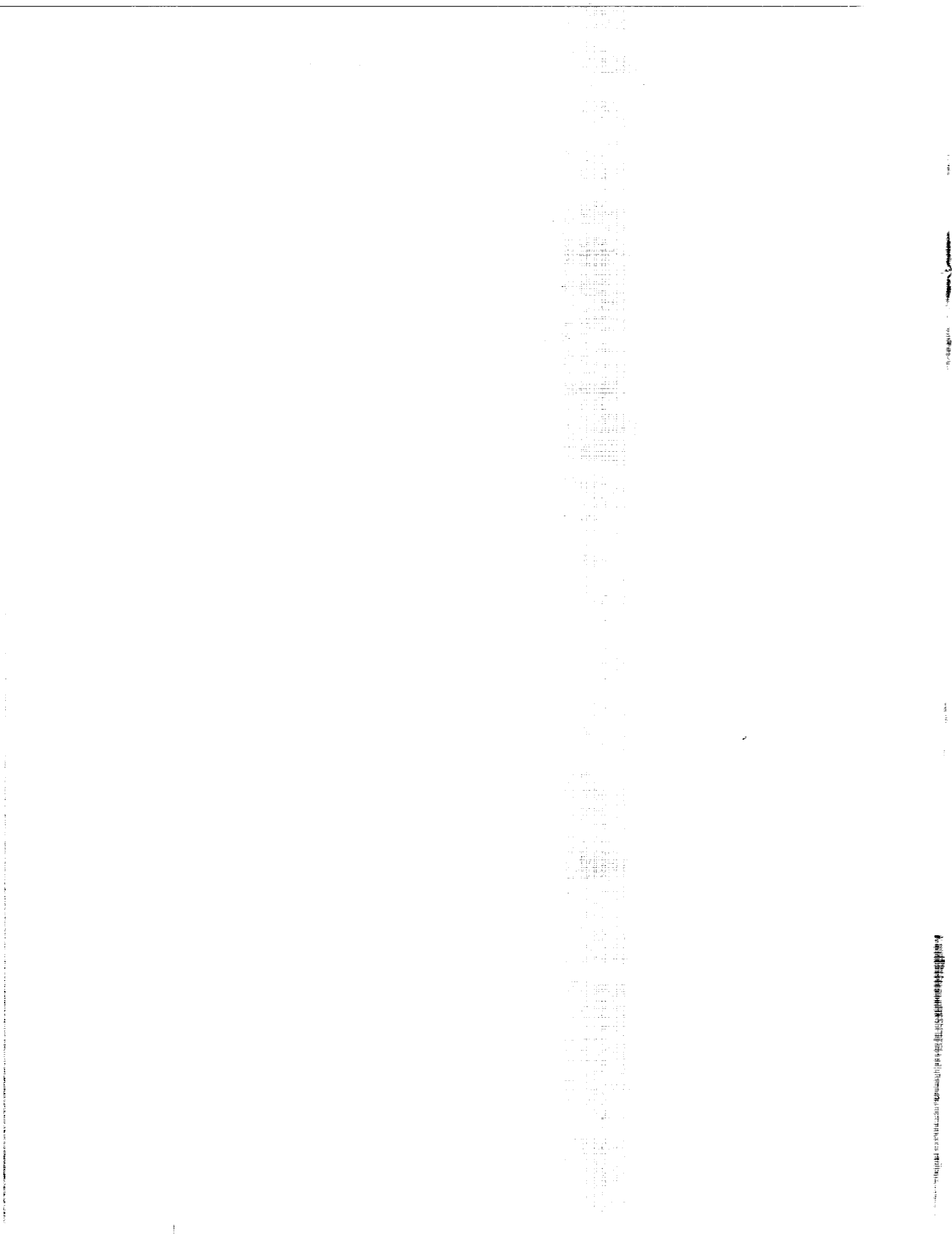
(NASA-EE-1181) SIMPLIFIED CURVE FITS FOR  
THE THERMODYNAMIC PROPERTIES OF EQUILIBRIUM  
AIR (NASA) 48 p Avail: MF01 FC A03/MF  
AC1 CSCL 20D

887-28309

H1/34 Unclass  
0095703



2



**NASA  
Reference  
Publication  
1181**

1987

# Simplified Curve Fits for the Thermodynamic Properties of Equilibrium Air

S. Srinivasan  
and J. C. Tannehill  
*Iowa State University  
Ames, Iowa*

K. J. Weilmuenster  
*Langley Research Center  
Hampton, Virginia*



National Aeronautics  
and Space Administration

Scientific and Technical  
Information Office



## Contents

Abstract . . . . .	1
Introduction . . . . .	1
Symbols . . . . .	1
Behavior of Air at High Temperature . . . . .	2
Sources of Equilibrium Air Properties . . . . .	2
Construction of Curve Fits . . . . .	3
Typical Curve Forms . . . . .	3
Transition Regions . . . . .	5
Equations of the Curve Fits . . . . .	8
$p = p(e, \rho)$ . . . . .	9
$a = a(e, \rho)$ . . . . .	9
$T = T(e, \rho)$ . . . . .	9
$h = h(p, \rho)$ . . . . .	10
$T = T(p, \rho)$ . . . . .	10
$s = s(e, \rho)$ . . . . .	10
$\rho = \rho(p, s)$ . . . . .	10
$e = e(p, s)$ . . . . .	11
$a = a(p, s)$ . . . . .	11
Results and Conclusions . . . . .	11
Appendix A Curve Fit Coefficients . . . . .	26
$p = p(e, \rho)$ . . . . .	26
$a = a(e, \rho)$ . . . . .	26
$T = T(e, \rho)$ . . . . .	26
$h = h(p, \rho)$ . . . . .	26
$T = T(p, \rho)$ . . . . .	26
$s = s(e, \rho)$ . . . . .	26
$\rho = \rho(p, s)$ . . . . .	26
$e = e(p, s)$ . . . . .	26
$a = a(p, s)$ . . . . .	26
Appendix B Master Program . . . . .	43
References . . . . .	44

PRECEDING PAGE BLANK NOT FILMED



## Abstract

New, improved curve fits for the thermodynamic properties of equilibrium air have been developed. The curve fits are for pressure, speed of sound, temperature, entropy, enthalpy, density, and internal energy. These curve fits can be readily incorporated into new or existing computational fluid dynamics codes if "real-gas" effects are desired. The curve fits are constructed from Grabau-type transition functions to model the thermodynamic surfaces in a piecewise manner. The accuracies and continuity of these curve fits are substantially improved over those of previous curve fits. These improvements are due to the incorporation of a small number of additional terms in the approximating polynomials and careful choices of the transition functions. The ranges of validity of the new curve fits are temperatures up to 25 000 K and densities from  $10^{-7}$  to  $10^3$  amagats.

## Introduction

Under subsonic flight conditions, air may be treated as an ideal gas composed of rigid rotating diatomic molecules. The thermodynamic properties of such a gas are well known. However, under hypersonic flight conditions, air may be raised to temperatures at which the molecules can no longer be treated as rigid rotators. Thus, there is a very real need for the thermodynamic and transport properties of equilibrium air for the computation of flow fields around bodies in high-speed flight. The references discussed below are representative of the various approaches for obtaining thermodynamic properties, but the list is by no means complete.

The thermodynamic properties of equilibrium air were calculated with good confidence as early as 1950. The earliest approach to compiling these properties was to present the information in the form of tables or charts (refs. 1 to 4).

Subsequently, equilibrium air thermodynamic properties became available in the form of FORTRAN computer programs. These programs can be broadly divided into two categories. The first category consists of programs that compute the equilibrium composition and thermodynamic properties using a harmonic-oscillator rigid-rotator model for the various component species of the gaseous mixture. Programs (refs. 5 to 8) were developed for the calculation of equilibrium properties of specific gas mixtures or of arbitrary chemical systems.

The second category of computer programs, which includes the present work, consists of programs that determine the thermodynamic properties of equilibrium air in a noniterative fashion using either interpolation or polynomial approximation techniques

(refs. 9 to 16). Typically, the sources of data for these programs are references 1 to 4. One such program, NASA RGAS (based on ref. 5), was an improvement over other sources of thermodynamic properties in terms of accuracy and range of validity. For this reason it is still widely used. The major shortcoming of the RGAS program is that the table lookup of coefficients for the cubic interpolation makes it too cumbersome and time-consuming to be efficiently used on an advanced computer.

Tannehill and associates (refs. 10, 15, and 16) developed simplified curve fits for the thermodynamic and transport properties of equilibrium air with the same range of validity as the NASA RGAS program. The curve fits were constructed through the use of Grabau-type transition functions in a manner similar to that of reference 11. In forming these curve fits, as many as five Grabau-type transition functions were joined with the perfect-gas equation of state.

One of the major shortcomings of the curve fits of references 10, 15, and 16 is the lack of continuity across the boundaries between the transition functions. As a consequence, numerical difficulties were sometimes encountered when these curve fits were employed in iterative flow-field computations. The primary objective of the present research was to alleviate this difficulty. At the same time, an attempt was made to improve the accuracy of the curve fits through incorporation of a small number of additional terms which would not significantly increase the computation time.

Through careful choice of the Grabau-type transition functions and use of complete bicubic polynomials, curve fits for pressure, speed of sound, temperature, entropy, enthalpy, density, and internal energy were developed and are presented herein. These curve fits are based on the NASA RGAS data and have the same ranges of validity, namely, temperatures up to 25 000 K and densities from  $10^{-7}$  to  $10^3$  amagats ( $\rho/\rho_0$ ).

## Symbols

$a$	speed of sound, m/s
$e$	specific internal energy, $\text{m}^2/\text{s}^2$
$h$	specific enthalpy, $\text{m}^2/\text{s}^2$
$p$	pressure, $\text{N}/\text{m}^2$
$R$	gas constant, $287.06 \text{ m}^2/\text{s}^2\text{-K}$
$s$	specific entropy, $\text{m}^2/\text{s}^2\text{-K}$
$T$	temperature, K
$\tilde{\gamma}$	$= h/e$

$\rho$  density, kg/m<sup>3</sup>

Subscript:

$o$  reference conditions at 1 atm and 273.15 K

## Behavior of Air at High Temperature

When a gas composed of polyatomic molecules is heated to high temperatures, its composition changes as a result of the chemical reactions which take place. Such a situation exists behind the shock wave which envelops a vehicle entering the atmosphere of the Earth. As a result of the change in chemical composition, the thermodynamic properties of the gas also change. When the temperature of the gas is raised appreciably higher than the temperature at which dissociation reactions begin to occur, the electrons receive energy quanta because of the collisions between atoms. If the temperature, and hence the kinetic energy of the atoms, is high enough so that electrons are removed from their orbits, ionization of the gas takes place. The effects of dissociation and ionization of the gas on its thermodynamic properties are often referred to as "real-gas" effects.

At room temperature, the volumetric composition of air is about 78 percent diatomic nitrogen, 21 percent diatomic oxygen, and about 1 percent argon and traces of carbon dioxide. When the temperature of air is raised above room temperature, deviations from perfect-gas behavior occur; that is, the vibrational mode of the molecules becomes excited, dissociation of both oxygen and nitrogen molecules occurs (although at different temperatures), nitric oxide is formed, and so forth. The chemical composition of air for densities lying between  $10^{-2}$  and 10 times normal air density is approximately divisible into the following regimes:

1.  $T < 2500$  K. The chemical composition is substantially that at room temperature.
2.  $2500 < T < 4000$  K. This is the oxygen dissociation regime; no significant nitrogen dissociation occurs; some NO is formed.
3.  $4000 < T < 8000$  K. This is the nitrogen dissociation regime; oxygen fully dissociates.
4.  $T > 8000$  K. Ionization of the atomic constituents occurs.

## Sources of Equilibrium Air Properties

The following discussion is intended to summarize the available mechanisms for determining equilibrium air properties. The cited references are not intended as a complete compilation but serve only as a listing typical of the various methods for determining the properties.

Prior to 1960, methods for determining equilibrium air properties were available only in summary form as tables or charts. The sources for information were the calculations of Gilmore (ref. 1), Hilsenrath and Beckett (ref. 2), Hansen (ref. 3), and Moeckel and Weston (ref. 4). In reference 3, data for compressibility factor, enthalpy, speed of sound, specific heat, Prandtl number, and the coefficients of viscosity and conductivity are presented as functions of temperature and pressure.

Eventually, the calculation of equilibrium air properties was possible through the use of FORTRAN computer programs, which can be divided broadly into two categories. The first category consists of programs that compute the equilibrium composition and thermodynamic properties using a harmonic-oscillator rigid-rotator model for the various component species of the gaseous mixture. Bailey (ref. 5) developed computer programs which used the temperature, density, and molar concentrations of the various constituent species to calculate the pressure, gas constant, enthalpy, entropy, specific heats, and coefficient of thermal conductivity. These properties were computed for a 9-species model as well as an 11-species model of equilibrium air. Zeleznik and Gordon (ref. 6) developed a sophisticated computer program, improved later by Gordon and McBride (ref. 7), which computed the chemical equilibrium composition of complex chemical systems given the constituent species and one of five possible pairs of thermodynamic state combinations. Also, a 27-reaction equilibrium air program was developed by Miner et al. (ref. 8).

The second category of computer programs consists of programs that determine the thermodynamic properties of equilibrium air in a noniterative fashion using either of the interpolation-of-polynomial approximation techniques. Lomax and Inouye (ref. 9) developed FORTRAN programs to determine the speed of sound, enthalpy, temperature, and entropy as functions of either pressure and density or pressure and entropy. Their programs used a 9-point spline interpolation and required a lookup of over 10000 tabulated values. The programs developed at NASA Ames Research Center in references 5 and 9 eventually evolved into the NASA RGAS program. The NASA RGAS program employs a cubic interpolation technique, with the associated table lookup of cubic coefficients, to compute the enthalpy, temperature, entropy, and speed of sound of 13 different gas mixtures, including equilibrium air as functions of either pressure and density, or pressure and entropy. The NASA RGAS program was modified by Tammehill and Mohling (ref. 10) to allow internal energy and density to be used as independent variables



for “time-dependent” flow calculations. The major shortcoming of the RGAS program is that the table lookup of coefficients for the cubic interpolation makes it too cumbersome and time-consuming to be efficiently employed on an advanced computer.

Among the first to develop programs which approximated the thermodynamic properties as self-contained closed-form expressions was Grabau (ref. 11). He outlined a systematic technique of modeling the thermodynamic properties with polynomial expressions containing exponential transitions. Using this technique, he determined the enthalpy, entropy, speed of sound, and compressibility of equilibrium air as functions of pressure and density in the form of closed-form expressions (curve fits). Using Grabau’s technique, Lewis and Burgess (ref. 12) obtained empirical equations for the density, enthalpy, speed of sound, and compressibility factor of air as functions of pressure and entropy. However, these curve fits had a range of validity only up to 15 000 K and a pressure range of 0.1 to 1.0 atm. The method of reference 11 was also employed by Barwell (ref. 13) to curve fit  $\tilde{\gamma}$  as a function of internal energy and density and temperature as a function of pressure and density for equilibrium air. Viegas and Howe (ref. 14) developed programs for the density, temperature, viscosity, and Prandtl number of equilibrium air as functions of pressure and enthalpy in the form of curve fits using least squares and Chebyshev polynomial fitting. Tannehill and associates (refs. 10, 15, and 16) developed simplified curve fits for the thermodynamic and transport properties of equilibrium air with the same range of validity as the NASA RGAS program. These curve fits included pressure, temperature, speed of sound, and coefficients of viscosity and thermal conductivity as functions of internal energy and density; also included were temperature and enthalpy as functions of pressure and density. The curve fits were constructed using Grabau-type transition functions in a manner similar to that of reference 11. In forming these curve fits, as many as five Grabau-type transition functions were joined with the perfect-gas equation of state.

## Construction of Curve Fits

### Typical Curve Forms

In the flow calculations of air in thermodynamic equilibrium, it becomes important to know the various thermodynamic properties as functions of a pair of independent state variables. In order to illustrate the spatial behavior of these thermodynamic surfaces, a typical curve is examined here in some detail. The nature of the thermodynamic surface, with the plausible reasons for its

undulating behavior, provides a qualitative insight into the choice of the approximating functions. Figure 1 shows the function  $\tilde{\gamma}$  plotted with respect to  $\log_{10}(p/p_0) - \log_{10}(\rho/\rho_0)$  at a density of  $10^{-7}$  amagats. Also shown are the various segments into which the curve may be divided, as indicated by A, AA, B, C, and D. These segments are basically quadratic or linear curves which are joined together by transition curves. Two types of transition curves appear in figure 1, and these are illustrated in figures 2 and 3. Figure 2 shows a transition function which passes through a point of inflection and is referred to as a transition with inflection. Figure 3 illustrates the second type of transition, which is one without a point of inflection. Figure 1 shows that  $\tilde{\gamma}$  goes through three distinct transitions with inflections. According to reference 3, there is a definite correlation between these three transitions and the change in chemical composition of the air as the temperature increases: the first transition, from AA to B, is due to the oxygen dissociation reaction; the second, from B to C, is due to the nitrogen dissociation; and the third, from C to D, is due to the ionization reactions.

In addition to the three transitions with inflections in figure 1, there appears to be a relatively insignificant transition without an inflection between curves A and AA. Also, after a careful examination of segment D, it appears that it may actually be part of an incomplete transition with a point of inflection.

The term  $\tilde{\gamma}$  is plotted as a function of  $\log_{10}(p/p_0) - \log_{10}(\rho/\rho_0)$  for various densities in figure 4, which includes the curve fit of figure 1. As the density increases, pieces of the curve near C and D disappear until only a part of the transition into C remains at  $10^3$  amagats. The reason for this is that the compressibility factor decreases steadily as the density is increased isothermally. Hence, it also follows that isothermal points move rapidly along the curve from D toward C as the density increases. Figure 4 provides an idea of the complexity of the problem of devising a practical method of modelling the collapse of the lower segments with increasing density. There appears to be a tendency for transitions with inflections to convert to transitions without inflections as the density increases. Reference 1 suggests that this conversion might be correlated with the simultaneous, abrupt increases of the concentrations of ionized oxygen and nitrogen atoms and of ionized nitrogen molecules.

As a consequence of the above discussion, one is motivated to model the thermodynamic surface, in a piecewise manner, with biquadratic or bicubic polynomials joined together by exponential transition functions with or without points of inflection. This is the procedure adopted in the present study.

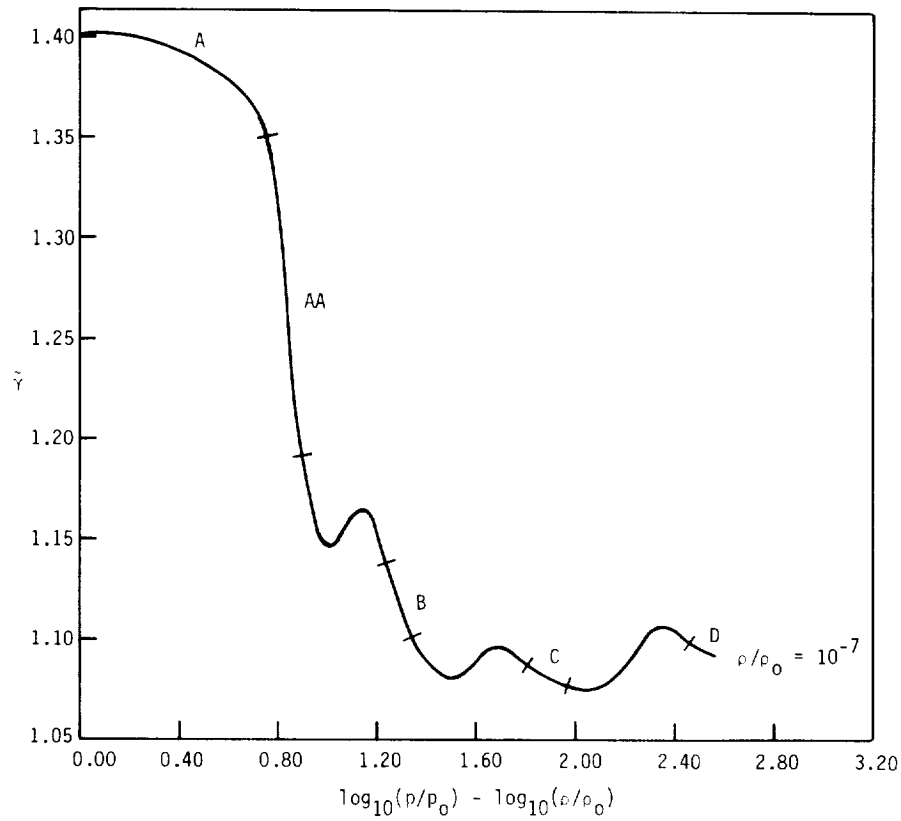


Figure 1. Variation of  $\tilde{\gamma}$  with  $\log_{10}(p/p_0) - \log_{10}(\rho/\rho_0)$  for  $\rho/\rho_0 = 10^{-7}$  amagats.

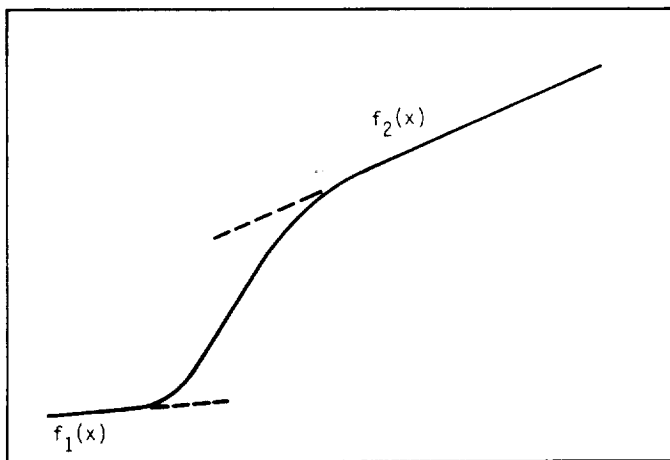


Figure 2. Transition curve with inflection.

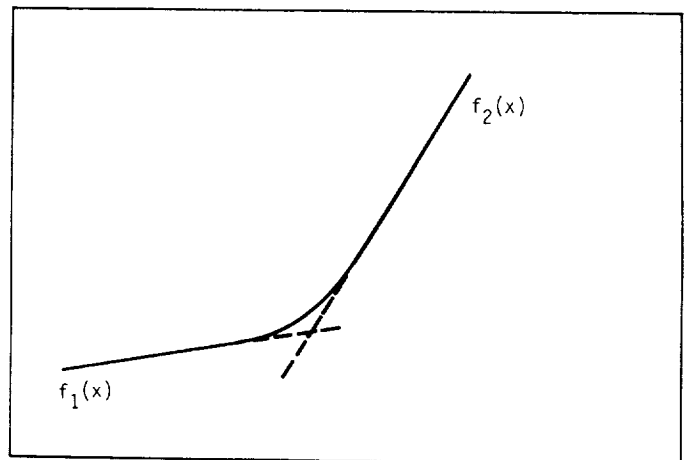


Figure 3. Transition curve without inflection.

## Transition Regions

The basic forms of the variables  $\tilde{\gamma}$  and  $\log_{10}(T/T_o)$ , plotted at constant densities as functions of  $\log_{10}(p/p_o) - \log_{10}(\rho/\rho_o)$ , are shown in figures 4 and 5. As mentioned previously, these curves exhibit segments of linear or quadratic functions successively connected by transition functions, which are asymptotic at both ends, and may or may not include points of inflection. The fact that at least some of these transitions can be attributed to dissociation phenomena suggests the use of exponential distribution functions.

Following the method outlined by Grabau (ref. 11), one has a choice of two kernel transition functions. The first is the Fermi-Dirac function

$$\frac{1}{1 + \exp(kx)} \quad (1)$$

which represents a transition between the levels zero and unity, where the direction and rate of the transition depend on the sign and the numerical magnitude of the exponential constant  $k$ . The numerator defines the upper level of the transition and may take on a variety of forms. In figure 6 the upper level of the transition is a straight line inclined to the horizontal, while the lower level is the  $x$ -axis. The transitions in figure 6 have points of inflection and, in the terminology of Grabau (ref. 11), are referred to as odd transitions.

The second type of transition function is the kernel of the Bose-Einstein distribution function

$$\frac{1}{1 - \exp(kx)} \quad (2)$$

which provides transitions leading from one function to another without a point of inflection and is obtained by merely changing the sign before the exponential term in the denominator of the Fermi-Dirac function. The transition function given by equation (2) is termed an even transition. Figure 7 illustrates two transitions of this kind between the  $x$ -axis and the line  $y = x$ , where (as before) the directions and rates of the transitions are governed by the sign and magnitude of the exponential constant  $k$ . It is important to note that the expression for an even transition becomes an indeterminate form when  $x$  is equal to the  $x$ -coordinate of the point of intersection of the two lines bounding the transition.

In the current study, each of the thermodynamic curves is approximated with quadratic or incomplete cubic segments connected by odd and even transitions as described above. Almost without exception, at low densities all the curves undergo odd transitions

which gradually diminish as the density increases and then change to even transitions. There are two ways of applying each of these transition functions. When the path of a curve appears to move from one straight line to another, there is an offset present which can be calculated in the direction of either of the variables. For accuracy it appears to be better to view the transition in terms of the smaller offset. Both ways of viewing the offsets involve the choice of a baseline. The use of the offset in the  $y$ -direction simplifies this choice since the  $x$ -axis serves as a natural baseline.

Consider the problem of determining the equation of a curve consisting of two linear segments connected by an odd transition function (fig. 8). The lower and upper line segments are given by

$$y_1 = a_1x + b_1 \quad (3)$$

and

$$y_2 = a_2x + b_2 \quad (4)$$

The  $y$  offset is their difference:

$$y_2 - y_1 = (a_2 - a_1)x + (b_2 - b_1) \quad (5)$$

which becomes the numerator of the transition function. The remaining constants of the transition function can be found graphically by drawing three lines between  $y_1$  and  $y_2$ . The median line is given by

$$y_o = \frac{y_1 + y_2}{2} \quad (6)$$

Let  $y_a$  be the median line between  $y_o$  and  $y_1$  and  $y_b$  be the corresponding median line between  $y_o$  and  $y_2$ . The center of the transition,  $(x_o, y_o)$ , is the point at which the transition crosses the median line  $y_o$ . The desired transition function is then of the form

$$y = y_1 + \frac{(a_2 - a_1)x + (b_2 - b_1)}{1 + \exp[k(x - x_o)]} \quad (7)$$

The exponential constant  $k$  is found from the coordinates  $x_a$  and  $x_b$  at which the transition intersects the lines  $y_a$  and  $y_b$ . Specifically, for the intersection with the line  $y_a$ ,

$$\frac{1}{1 + \exp[k(x_a - x_o)]} = \frac{1}{4} \quad (8)$$

so that

$$\exp[k(x_a - x_o)] = 3 \quad (9)$$

Solving for  $k$  yields

$$k = \frac{\ln 3}{x_a - x_o} \quad (10)$$

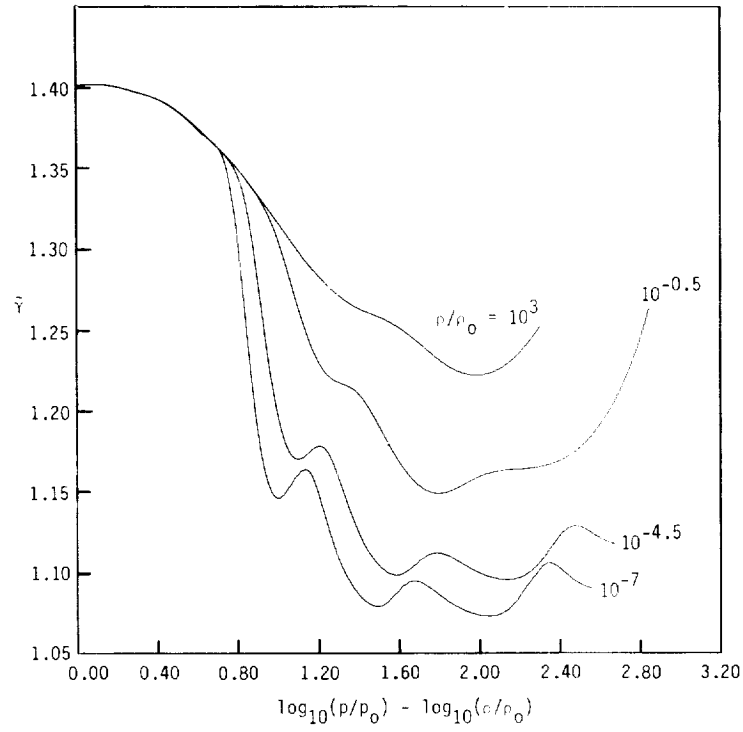


Figure 4. Variation of  $\tilde{\gamma}$  with  $\log_{10}(p/p_0) - \log_{10}(\rho/\rho_0)$  for various densities.

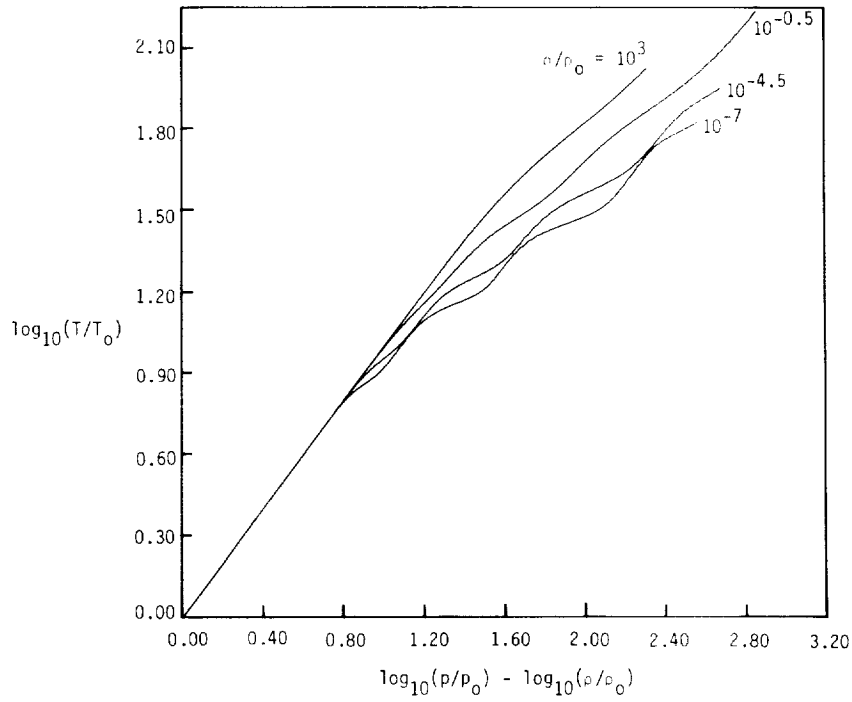


Figure 5. Variation of  $\log_{10}(T/T_0)$  with  $\log_{10}(p/p_0) - \log_{10}(\rho/\rho_0)$  for various densities.

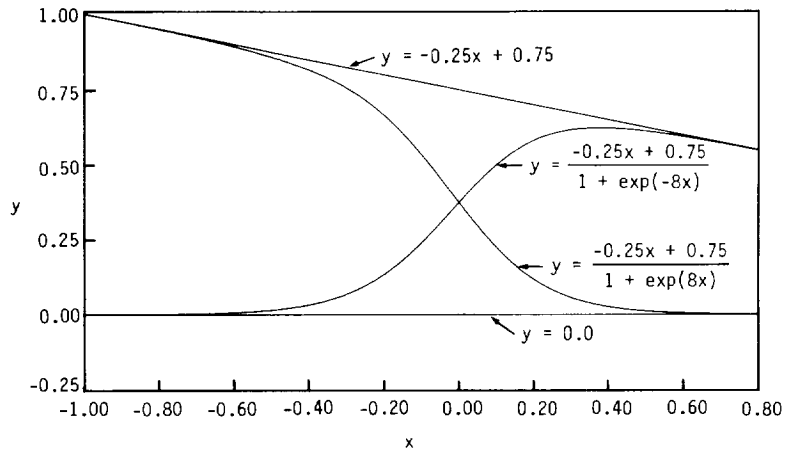


Figure 6. Two odd transition functions.

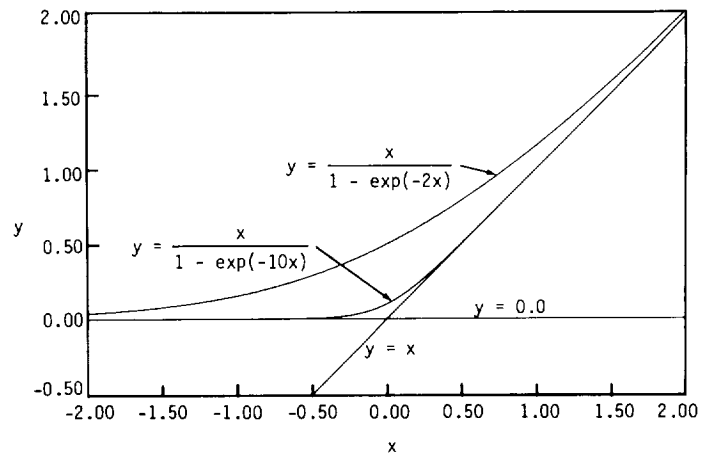


Figure 7. Two even transition functions.

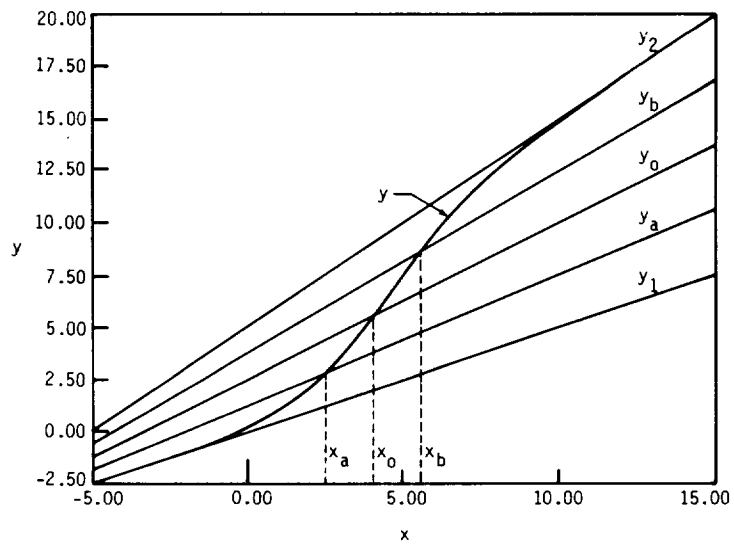


Figure 8. Construction of an odd transition function.

From the intersection of  $y$  with  $y_b$  we get

$$k = \frac{\ln 3}{x_o - x_b} \quad (11)$$

This procedure obviously yields two numerical values for the constant  $k$ . However, they are substantially alike in most instances.

The determination of the constants of an even transition is simpler. In terms of the  $y$  offset, such a transition can be written in the form

$$y = \frac{a(x - x_o)}{1 - \exp[k(x - x_o)]} \quad (12)$$

where  $x_o$  is the  $x$ -coordinate of the point of intersection of the two lines bounding the transition. The value of the exponential constant  $k$  follows from the coordinate  $y_o$  at  $x = x_o$ . Since the expression for  $y$  is an indeterminate form at this point, its value is given by the ratio of the derivatives of the numerator and of the denominator at this point:

$$y_o = \frac{x^{\lim \rightarrow x_o} \left\{ \frac{d}{dx} [a(x - x_o)] \right\}}{x^{\lim \rightarrow x_o} \left\{ \frac{d}{dx} [1 - \exp[k(x - x_o)]] \right\}} \quad (13)$$

which gives

$$k = \frac{-a}{y_o} \quad (14)$$

This approach for determining the constants of the Grabau-type transitions is extended in the present work to approximate transitions in two independent variables. The kernel of an odd transition function in three dimensions is

$$\frac{1}{1 + \exp(a_o + a_1x + a_2y + a_3xy)} \quad (15)$$

which is essentially an alternate form of

$$\frac{1}{1 + \exp[k(x - x_o)(y - y_o)]} \quad (16)$$

Equation (15) is more convenient for determining the values of the constants  $a_0$  to  $a_3$  as dictated by the behavior imposed on the transition function. The general technique of determining the values of these constants differs from the approach outlined earlier and is as follows. The boundaries of the transition in the directions of the two independent variables are  $x_a \leq x \leq x_b$  and  $y_c \leq y \leq y_d$ . If  $f_1(x, y)$  and  $f_2(x, y)$  are the two surfaces limiting the transition function  $f(x, y)$ , then

$$f(x, y) = f_1(x, y) + \frac{f_2(x, y) - f_1(x, y)}{1 + \exp(a_o + a_1x + a_2y + a_3xy)} \quad (17)$$

In order to ensure an accurate and smooth transition from  $f_1(x, y)$  to  $f_2(x, y)$ , we require the quadratic expression  $(a_0 + a_1x + a_2y + a_3xy)$  to behave as follows. At the lower left corner point  $(x_a, y_c)$  the quadratic expression should have a large positive value so that  $f(x, y) \approx f_1(x, y)$ . At the upper right corner point  $(x_b, y_d)$  the quadratic expression should have a large negative value in order to ensure that  $f(x, y) \approx f_2(x, y)$ . At the midpoints of the left and right boundaries,  $[x_a, (y_c + y_d)/2]$  and  $[x_b, (y_c + y_d)/2]$ , respectively, the quadratic expression should be zero so that

$$f(x, y) \approx \frac{f_1(x, y) + f_2(x, y)}{2}$$

These conditions yield the following four linear equations:

$$a_0 + a_1x_a + a_2y_c + a_3x_ax_c = +k \quad (18)$$

$$a_0 + a_1x_b + a_2y_d + a_3x_bx_d = -k \quad (19)$$

$$a_0 + a_1x_a + a_2(y_c + y_d)/2 + a_3x_a(y_c + y_d)/2 = 0 \quad (20)$$

$$a_0 + a_1x_b + a_2(y_c + y_d)/2 + a_3x_b(y_c + y_d)/2 = 0 \quad (21)$$

where  $k$  is a positive constant (typically  $20 \leq k \leq 25$ ) chosen such that  $\exp(k)$  and  $\exp(-k)$  do not yield overflow and underflow conditions on a computer. The constants  $a_0$  to  $a_3$  can now be obtained in a straightforward manner from the system of four linear equations in four unknowns (eqs. (18) to (21)).

The above method of obtaining the Grabau-type transition functions proved quite accurate in ensuring a negligible mismatch in the dependent variable over the boundaries of adjoining subregions. It is a merit of this stepwise method of constructing empirical equations that any part can be removed for corrections without disturbing the surface approximation as a whole.

## Equations of the Curve Fits

The curve fits for the various thermodynamic properties are constructed through use of Grabau-type transition functions, as described previously. The general form of these curve fits can be written as

$$z(x, y) = f_1(x, y) + \frac{f_2(x, y) - f_1(x, y)}{1 \pm \exp(k_0 + k_1x + k_2y + k_3xy)} \quad (22)$$

where, in general,

$$f_1(x, y) = p_1 + p_2x + p_3y + p_4xy + p_5x^2 + p_6y^2 + p_7x^2y + p_8xy^2 + p_9x^3 + p_{10}y^3 \quad (23)$$

and

$$f_2(x, y) - f_1(x, y) = p_{11} + p_{12}x + p_{13}y + p_{14}xy + p_{15}x^2 + p_{16}y^2 + p_{17}x^2y + p_{18}xy^2 + p_{19}x^3 + p_{20}y^3 \quad (24)$$

The coefficients  $k_0$  to  $k_3$  in the denominator of the transition function in equation (22) are determined by the technique outlined in the preceding section. The coefficients  $p_1$  to  $p_{20}$  in equations (23) and (24) are determined by the actual curve fitting of the data from the NASA RGAS program. The exact location and number of these data points over the curve fit domain determines the accuracy of the curve fits. The points are clustered near the boundaries of the domain and the middle region of the transition in order to ensure continuity at the boundaries and accuracy within the domain. The data from the NASA RGAS program are fitted to the equations of the curve fits by the method of least squares. A multiple linear regression technique (ref. 17) is used to determine the coefficients  $p_1$  to  $p_{20}$ .

The general form of the curve fit for each thermodynamic property is described below. As in references 10 and 15, for each of the curve fits where density is one of the independent variables, the range of  $\rho$  is subdivided into three separate regions, with different coefficients being used in the curve fits for each region (fig. 9). The division lines are located at  $\log_{10}(\rho/\rho_0) = -4.5$  and  $\log_{10}(\rho/\rho_0) = -0.5$ .

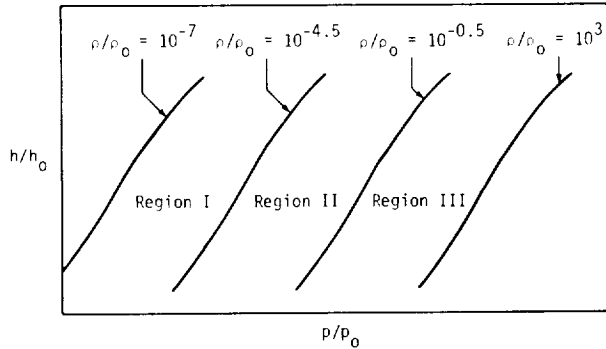


Figure 9. Division of curve fit range by density.

In order to ensure continuity of the dependent variables across these two division lines the following technique was adopted. If the choice of independent variables yields a point within a specified band about either of these division lines, the dependent variable is linearly interpolated between the values obtained at the endpoints of the band. The coefficients for all the curve fits have been tabulated in appendix A. In appendix B, a master program which handles all the thermodynamic computations is described and a reference is cited for a listing of the

computer program.

$$p = p(e, \rho)$$

For the correlation of  $p = p(e, \rho)$ , the ratio  $\tilde{\gamma} = h/e$  is curve fitted as a function of  $e$  and  $\rho$  so that  $p$  can be calculated from

$$p = \rho e(\tilde{\gamma} - 1) \quad (25)$$

The general form of the equation used for  $\tilde{\gamma}$  is

$$\begin{aligned} \tilde{\gamma} = & a_1 + a_2Y + a_3Z + a_4YZ + a_5Y^2 \\ & + a_6Z^2 + a_7Y^2Z + a_8YZ^2 + a_9Y^3 \\ & + a_{10}Z^3 + (a_{11} + a_{12}Y + a_{13}Z \\ & + a_{14}YZ + a_{15}Y^2 + a_{16}Z^2 + a_{17}Y^2Z \\ & + a_{18}YZ^2 + a_{19}Y^3 + a_{20}Z^3)/[1 \pm \exp(a_{21} \\ & + a_{22}Y + a_{23}Z + a_{24}YZ)] \end{aligned} \quad (26)$$

where  $Y = \log_{10}(\rho/\rho_0)$  and  $Z = \log_{10}(e/RT_0)$ . The units for  $\rho$  are  $\text{kg}/\text{m}^3$  and the units for  $e$  are  $\text{m}^2/\text{s}^2$ . It should be noted that not all the terms appearing in the above equation are used over the complete range of  $e$  and  $\rho$ .

$$a = a(e, \rho)$$

An exact expression for the speed of sound  $a$  in terms of  $\tilde{\gamma}$  was derived by Barnwell (ref. 13) and may be written as

$$a = \left( e \left\{ (\tilde{\gamma} - 1) \left[ \tilde{\gamma} + \left( \frac{\partial \tilde{\gamma}}{\partial \ln e} \right)_{\rho} \right] + \left( \frac{\partial \tilde{\gamma}}{\partial \ln \rho} \right)_{e} \right\} \right)^{1/2} \quad (27)$$

Since complete bicubic polynomials are used for  $f_1(Y, Z)$  and  $f_2(Y, Z) - f_1(Y, Z)$  in equation (26) for  $\tilde{\gamma}$ , equation (27) is used directly for the correlation  $a = a(e, \rho)$  without further corrections, unlike in references 10 and 15. The expressions for  $\left( \frac{\partial \tilde{\gamma}}{\partial \ln e} \right)_{\rho}$  and  $\left( \frac{\partial \tilde{\gamma}}{\partial \ln \rho} \right)_{e}$  are presented in appendix A.

$$T = T(e, \rho)$$

In the calculation of  $T = T(e, \rho)$ , the pressure is first determined with equation (25), and then the temperature is calculated with the equation

$$\begin{aligned} \log_{10}(T/T_0) = & b_1 + b_2Y + b_3Z + b_4YZ + b_5Y^2 + b_6Z^2 \\ & + b_7Y^2Z + b_8YZ^2 + b_9Y^3 + b_{10}Z^3 \\ & + (b_{11} + b_{12}Y + b_{13}Z + b_{14}YZ \\ & + b_{15}Y^2 + b_{16}Z^2 + b_{17}Y^2Z + b_{18}YZ^2 \\ & + b_{19}Y^3 + b_{20}Z^3)/[1 + \exp(b_{21} \\ & + b_{22}Y + b_{23}Z + b_{24}YZ)] \end{aligned} \quad (28)$$

where  $Y = \log_{10}(\rho/\rho_0)$ ,  $X = \log_{10}(p/p_0)$ , and  $Z = X - Y$ . The units for  $p$  are  $\text{N}/\text{m}^2$ , and the units for

$T$  are K. The coefficients  $b_1$  to  $b_{24}$  are determined in such a way as to compensate for the errors incurred in the initial calculation of pressure with equation (25).

$$h = h(p, \rho)$$

For the correlation of  $h = h(p, \rho)$ , the ratio  $\tilde{\gamma} = h/e$  is curve fitted as a function of  $p$  and  $\rho$  so that  $h$  can be calculated from

$$h = (p/\rho)[\tilde{\gamma}/(\tilde{\gamma} - 1)] \quad (29)$$

The general form of the equation used for  $\tilde{\gamma}$  is

$$\begin{aligned} \tilde{\gamma} = & c_1 + c_2Y + c_3Z + c_4YZ + c_5Y^2 \\ & + c_6Z^2 + c_7Y^2Z + c_8YZ^2 \\ & + c_9Y^3 + c_{10}Z^3 + (c_{11} + c_{12}Y \\ & + c_{13}Z + c_{14}YZ + c_{15}Y^2 + c_{16}Z^2 \\ & + c_{17}Y^2Z + c_{18}YZ^2 + c_{19}Y^3 \\ & + c_{20}Z^3)/[1 \pm \exp(c_{21} + c_{22}Y \\ & + c_{23}Z + c_{24}YZ)] \end{aligned} \quad (30)$$

where  $Y = \log_{10}(\rho/\rho_0)$ ,  $X = \log_{10}(p/p_0)$ , and  $Z = X - Y$ . For the correlations  $p = p(e, \rho)$  and  $h = h(p, \rho)$ , where  $\tilde{\gamma}$  is the variable curve fitted, an even transition function is used to model the transition between the perfect-gas equation and the remainder of the curve fit in the lowest density region ( $-7.0 \leq \log_{10}(\rho/\rho_0) \leq -4.50$ ). This yields a more accurate fit than an ordinary bicubic curve without any transitions.

$$T = T(p, \rho)$$

The general form of the equation used for the correlation  $T = T(p, \rho)$  is

$$\begin{aligned} \log_{10}(T/T_0) = & d_1 + d_2Y + d_3Z \\ & + d_4YZ + d_5Y^2 + d_6Z^2 + d_7Y^2Z \\ & + d_8YZ^2 + d_9Y^3 + d_{10}Z^3 \\ & + (d_{11} + d_{12}Y + d_{13}Z + d_{14}YZ \\ & + d_{15}Y^2 + d_{16}Z^2 + d_{17}Y^2Z \\ & + d_{18}YZ^2 + d_{19}Y^3 + d_{20}Z^3)/[1 + \exp(d_{21} \\ & + d_{22}Y + d_{23}Z + d_{24}YZ)] \end{aligned} \quad (31)$$

where  $Y = \log_{10}(\rho/\rho_0)$ ,  $X = \log_{10}(p/p_0)$ , and  $Z = X - Y$ .

$$s = s(e, \rho)$$

For the correlation of  $s = s(e, \rho)$ , the general form of the equation used is

$$\begin{aligned} \frac{s}{R} = & e_1 + e_2Y + e_3Z + e_4YZ + e_5Y^2 + e_6Z^2 \\ & + e_7Y^2Z + e_8YZ^2 + e_9Y^3 + e_{10}Z^3 \end{aligned} \quad (32)$$

where  $Y = \log_{10}(\rho/\rho_0)$  and  $Z = \log_{10}(e/RT_0)$ . The units for  $s$  are  $\text{m}^2/\text{s}^2\text{-K}$ . As is evident from equation (32), Grabau transition functions are not necessary for this curve fit.

$$\rho = \rho(p, s)$$

Unlike the preceding curve fits in which density is one of the independent variables, the domain of the curve fit  $\rho = \rho(p, s)$ , as well as the curve fits  $e = e(p, s)$  and  $a = a(p, s)$ , cannot be divided into subdomains on the basis of density. For reasons of accuracy, it is necessary to subdivide the domain in terms of  $s$  as shown in figure 10.

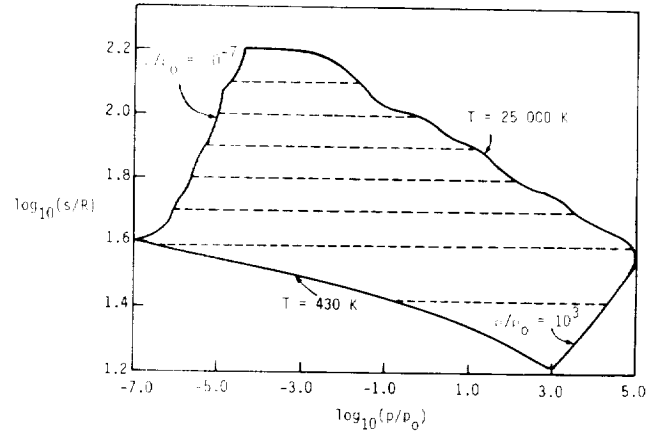


Figure 10. Division of curve fit range by entropy.

The general form of the equation used for the correlation of  $\rho = \rho(p, s)$  is

$$\begin{aligned} \log_{10}(\rho/\rho_0) = & f_1 + f_2Y + f_3Z + f_4YZ + f_5Y^2 \\ & + f_6Z^2 + f_7Y^2Z + f_8YZ^2 \\ & + f_9Y^3 + f_{10}Z^3 + (f_{11} + f_{12}Y \\ & + f_{13}Z + f_{14}YZ + f_{15}Y^2 + f_{16}Z^2 \\ & + f_{17}Y^2Z + f_{18}YZ^2 + f_{19}Y^3 \\ & + f_{20}Z^3)/[1 + \exp(f_{21} \\ & + f_{22}Y + f_{23}Z + f_{24}X + f_{25}Y^2)] \end{aligned} \quad (33)$$

where  $Y = \log_{10}(s/R)$ ,  $X = \log_{10}(p/p_0)$ , and  $Z = X - Y$ . The units for  $s$  are  $\text{m}^2/\text{s}^2\text{-K}$ .



$$e = e(p, s)$$

For the correlation of  $e = e(p, s)$ , the general form of the curve fit equation is

$$\begin{aligned} \log_{10}(e/RT_0) = & g_1 + g_2Y + g_3Z + g_4YZ \\ & + g_5Y^2 + g_6Z^2 + g_7Y^2Z \\ & + g_8YZ^2 + g_9Y^3 + g_{10}Z^3 \\ & + (g_{11} + g_{12}Y + g_{13}Z + g_{14}YZ \\ & + g_{15}Y^2 + g_{16}Z^2 + g_{17}Y^2Z \\ & + g_{18}YZ^2 + g_{19}Y^3 + g_{20}Z^3)/[1 + \exp(g_{21} \\ & + g_{22}Y + g_{23}Z + g_{24}X + g_{25}Y^2)] \quad (34) \end{aligned}$$

where  $Y = \log_{10}(s/R)$ ,  $X = \log_{10}(p/p_0)$ , and  $Z = X - Y$ .

$$a = a(p, s)$$

For the correlation of  $a = a(p, s)$ , the general form of the equation is

$$\begin{aligned} \log_{10}(a/a_0) = & h_1 + h_2Y + h_3Z + h_4YZ \\ & + h_5Y^2 + h_6Z^2 + h_7Y^2Z + h_8YZ^2 \\ & + h_9Y^3 + h_{10}Z^3 + (h_{11} + h_{12}Y \\ & + h_{13}Z + h_{14}YZ + h_{15}Y^2 \\ & + h_{16}Z^2 + h_{17}Y^2Z + h_{18}YZ^2 \\ & + h_{19}Y^3 + h_{20}Z^3)/[1 + \exp(h_{21} \\ & + h_{22}Y + h_{23}Z + h_{24}X + h_{25}Y^2)] \quad (35) \end{aligned}$$

where  $Y = \log_{10}(s/R)$ ,  $X = \log_{10}(p/p_0)$ , and  $Z = X - Y$ . The units of  $a$  are m/s.

## Results and Conclusions

New, simplified curve fits for the thermodynamic properties of equilibrium air were constructed with the procedures described in the preceding sections. Comparisons of the curve fits  $p = p(e, \rho)$ ,  $a = a(e, \rho)$ ,  $T = T(e, \rho)$ ,  $s = s(e, \rho)$ ,  $T = T(p, \rho)$ ,  $h = h(p, \rho)$ ,  $\rho = \rho(p, s)$ ,  $e = e(p, s)$ , and  $a = a(p, s)$  with the original NASA RGAS program are shown in figures 11 to 19. The following procedure was employed in making the comparisons for the first four curve fits. First,  $p$  and  $\rho$  data were supplied as input to the NASA RGAS program and  $e$  was computed. Then, this  $e$  and the original  $\rho$  were used to obtain  $p$ ,  $a$ ,  $T$ , and  $s$  from the above curve fits. As a result of this procedure,  $\log_{10}(p/p_0)$  is plotted as one of the independent variables in figures 11 to 14. The same  $p$  and  $\rho$  data used above were also employed in the comparisons for the curve fits  $T = T(p, \rho)$  and  $h = h(p, \rho)$ .

The method adopted for the comparisons of  $\rho = \rho(p, s)$ ,  $e = e(p, s)$ , and  $a = a(p, s)$  with the NASA

RGAS program was quite similar to that for the first four curve fits. First,  $p$  and  $\rho$  were supplied to the NASA RGAS program, which yielded  $s$ . This  $s$  and the original  $p$  were used in the above curve fits to obtain  $\rho$ ,  $e$ , and  $a$ .

The above comparisons are presented graphically to provide a qualitative overview of the accuracy of the curve fits. However, as figures 11 to 19 indicate, these graphical comparisons are restricted to points lying on 11 constant-density lines ranging from  $10^{-7}$  to  $10^3$  amagats. In order to ensure the validity and accuracy of the curve fits across the entire domain, a more comprehensive accuracy test was carried out. The new curve fits were compared with the NASA RGAS program for relative accuracies at approximately 22 000 data points. These test points were chosen to span the entire density range from  $10^{-7}$  to  $10^3$  amagats and temperatures varying from 273 K to 25 000 K. The results of these comprehensive accuracy checks are presented in tables 1 to 9. For the curve fits  $p = p(e, \rho)$ ,  $a = a(e, \rho)$ ,  $T = T(e, \rho)$ ,  $T = T(p, \rho)$ , and  $h = h(p, \rho)$ , comparisons with the curve fits of reference 15 are also presented in the tables. The first column in the tables represents the percentage error in the comparison of a property generated by the RGAS program and a curve fit. The other columns contain the percentage of points in the test data base, generated by a curve fit, which are in error by an amount greater than that indicated in column 1. The accuracies of the present curve fits are substantially improved over the accuracies of the previous curve fits appearing in reference 15. The somewhat higher percentage errors in the curve fits with  $p$  and  $s$  as independent variables can be attributed to the fact that a line of constant  $s$  spans the entire density range, sometimes necessitating the use of two Grabau-type transition functions. Requiring a minimal mismatch across the junctions of these transition functions resulted in a relative loss of accuracy. However, these latter curve fits are well within the accuracy limits required for most engineering applications.

One of the primary objectives of this research was to minimize the discontinuities in the dependent variables across juncture points of the curve fits (fig. 20). Comparisons of the dependent variables at juncture points of the curve fits for  $p = p(e, \rho)$ ,  $a = a(e, \rho)$ ,  $T = T(e, \rho)$ ,  $T = T(p, \rho)$ , and  $h = h(p, \rho)$  are presented in tables 10 to 14. These new curve fits showed a substantial improvement in continuity at the juncture points when compared with the previous curve fits. For the curve fits where  $p$  and  $s$  were the independent variables, it was very difficult to maintain continuity at the juncture points. This was due to the manner in which

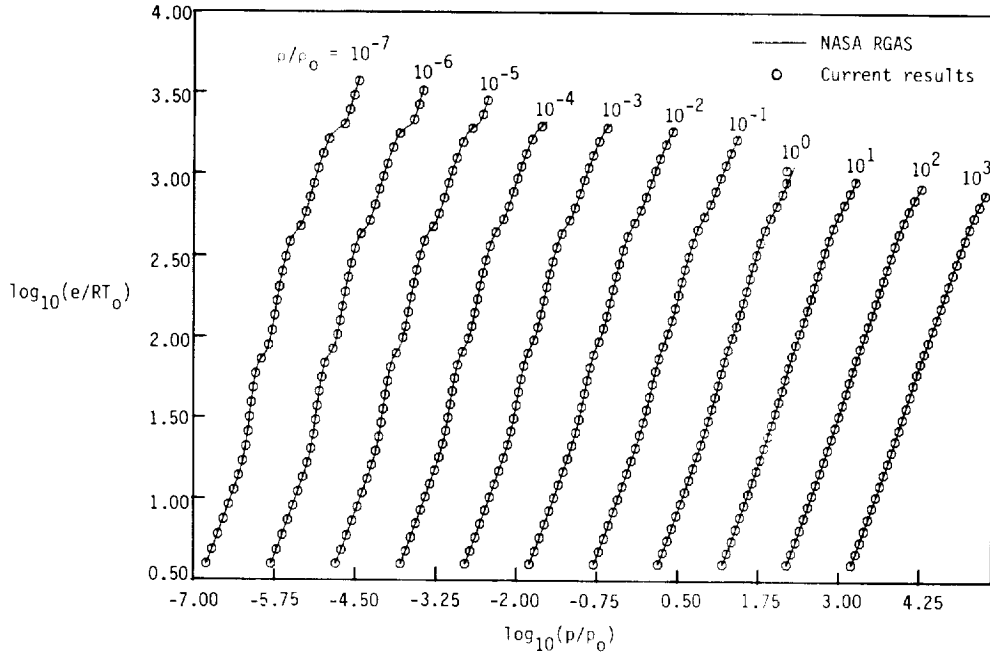


Figure 11. Comparison of curve fits for  $p = p(e, \rho)$ .

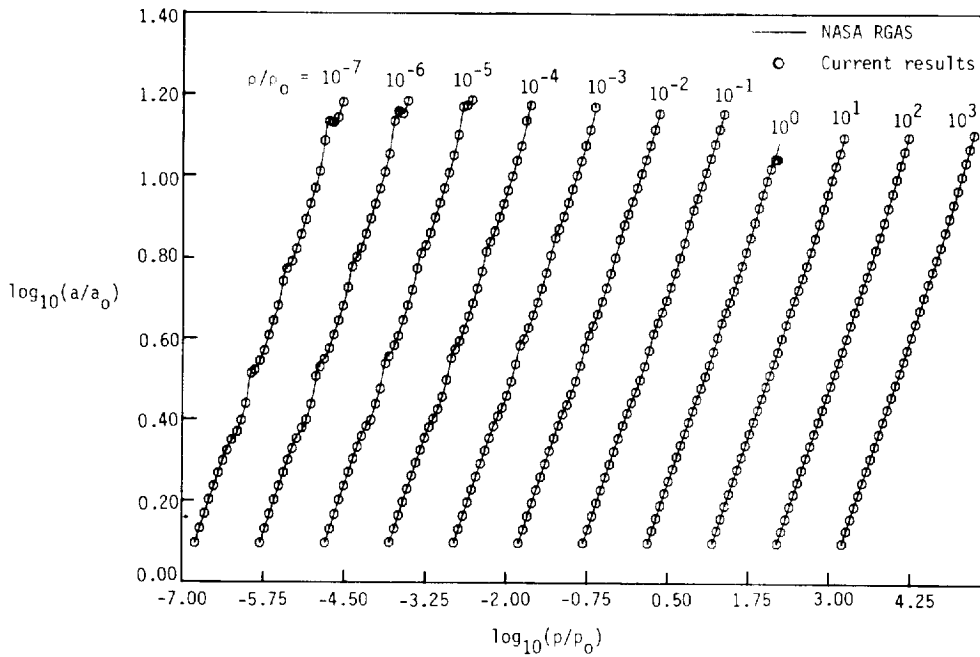


Figure 12. Comparison of curve fits for  $a = a(e, \rho)$ .

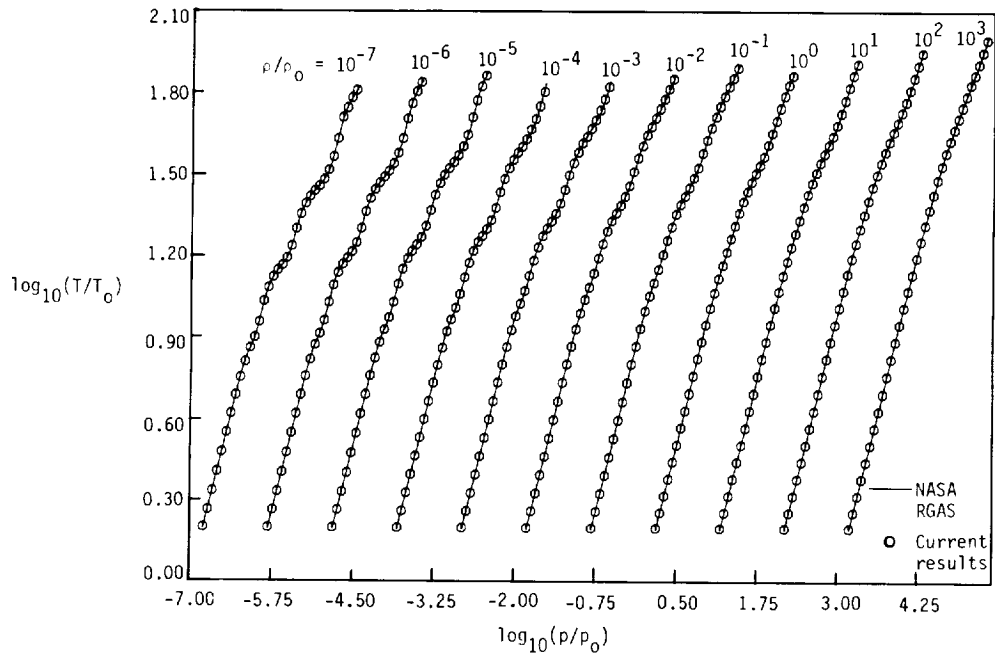


Figure 13. Comparison of curve fits for  $T = T(e, \rho)$ .

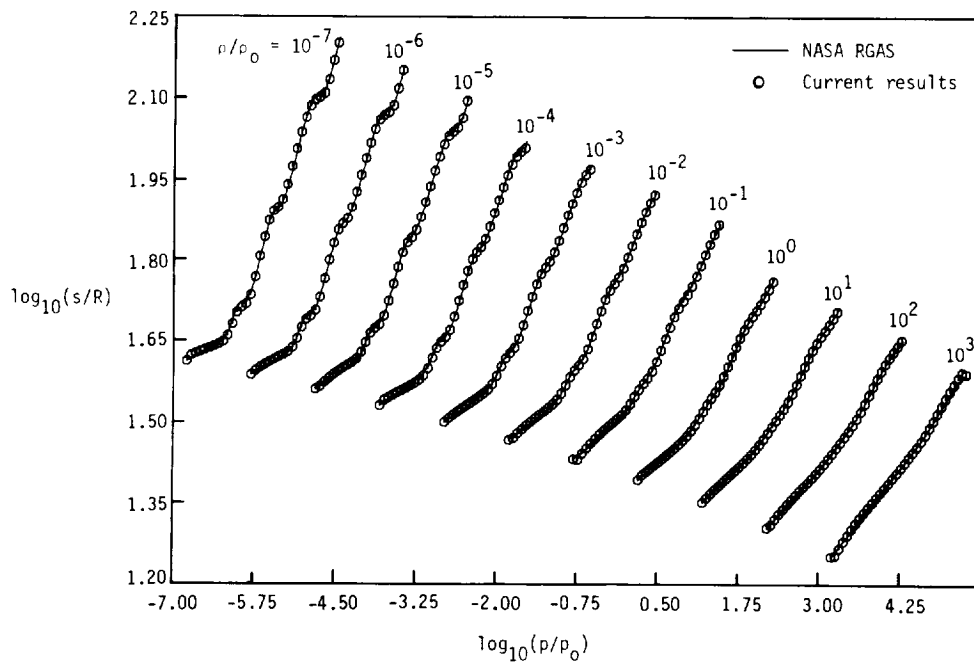


Figure 14. Comparison of curve fits for  $s = s(e, \rho)$ .

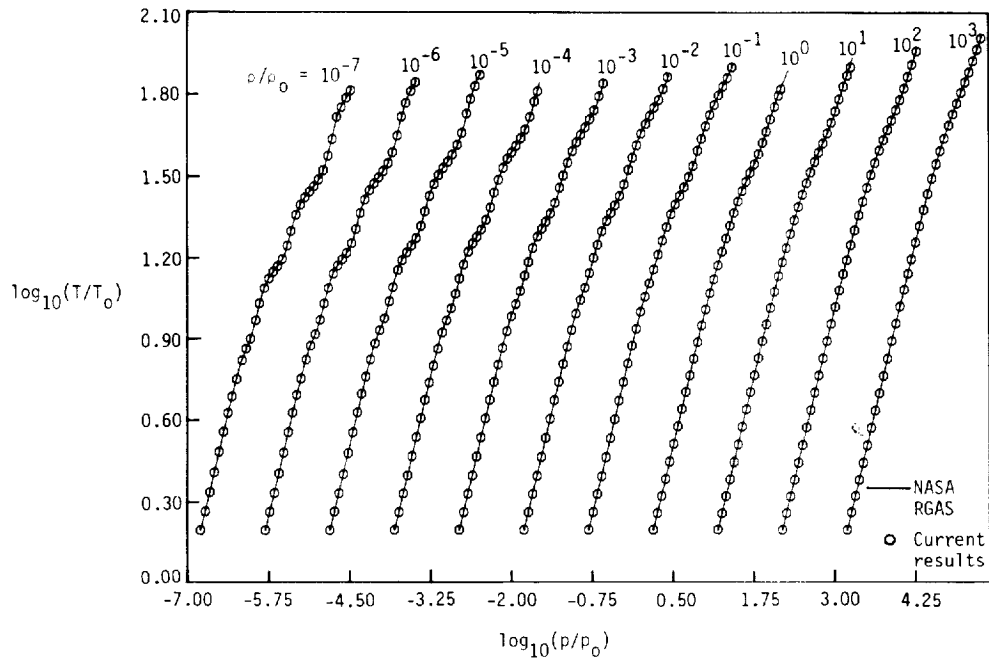


Figure 15. Comparison of curve fits for  $T = T(p, \rho)$ .

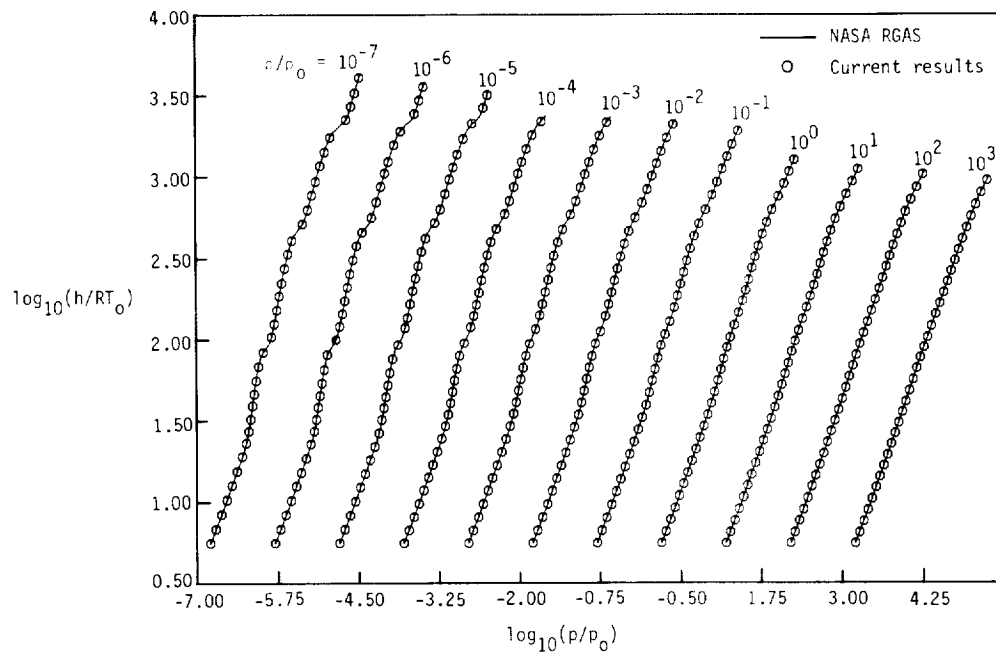


Figure 16. Comparison of curve fits for  $h = h(p, \rho)$ .

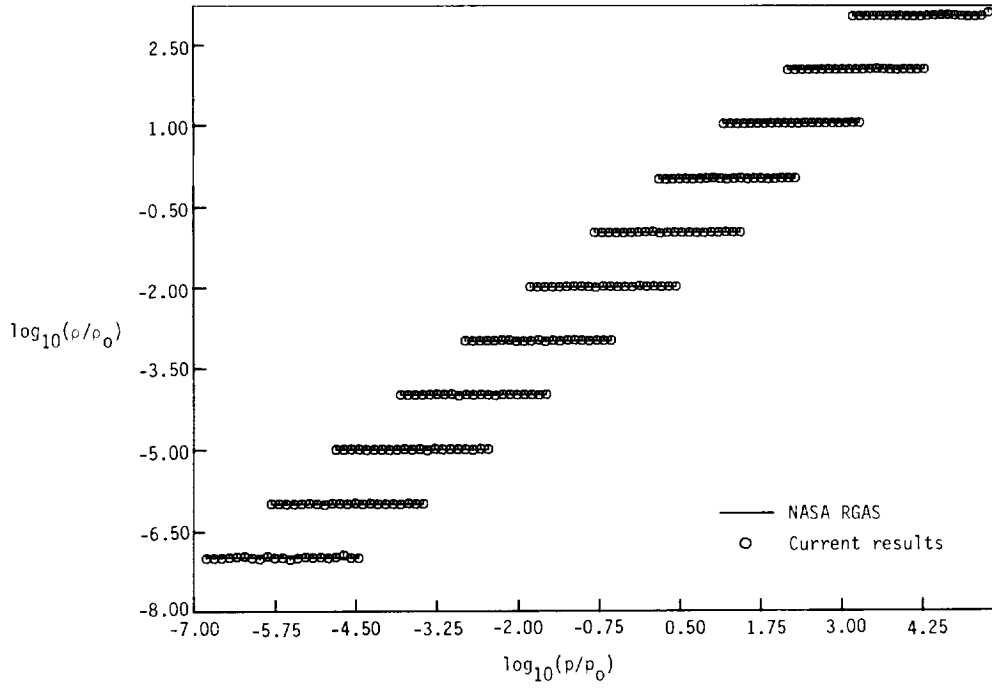


Figure 17. Comparison of curve fits for  $\rho = \rho(p, s)$ .

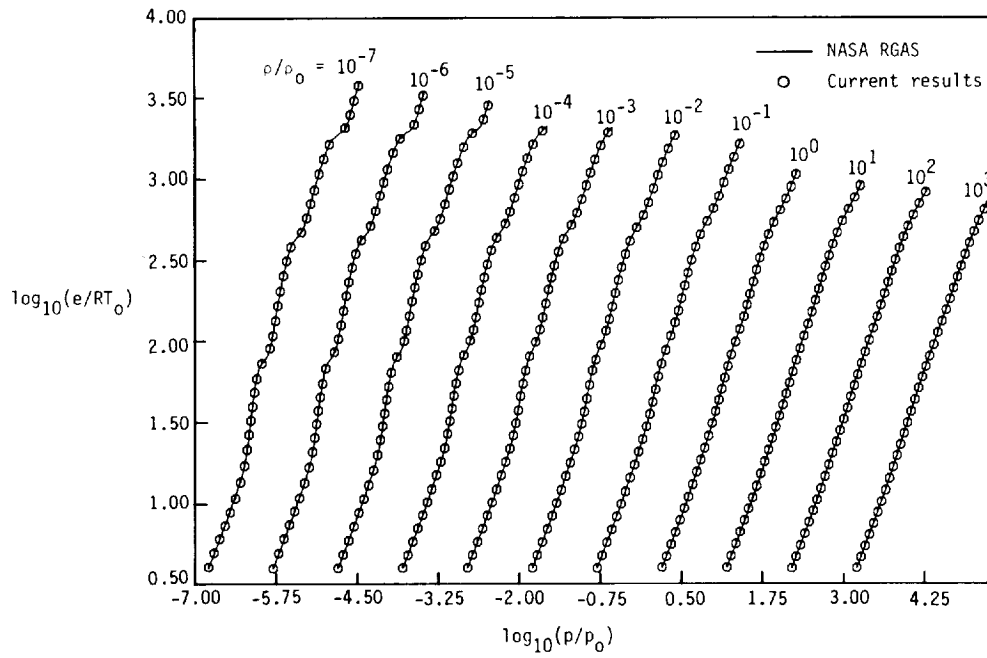


Figure 18. Comparison of curve fits for  $e = e(p, s)$ .

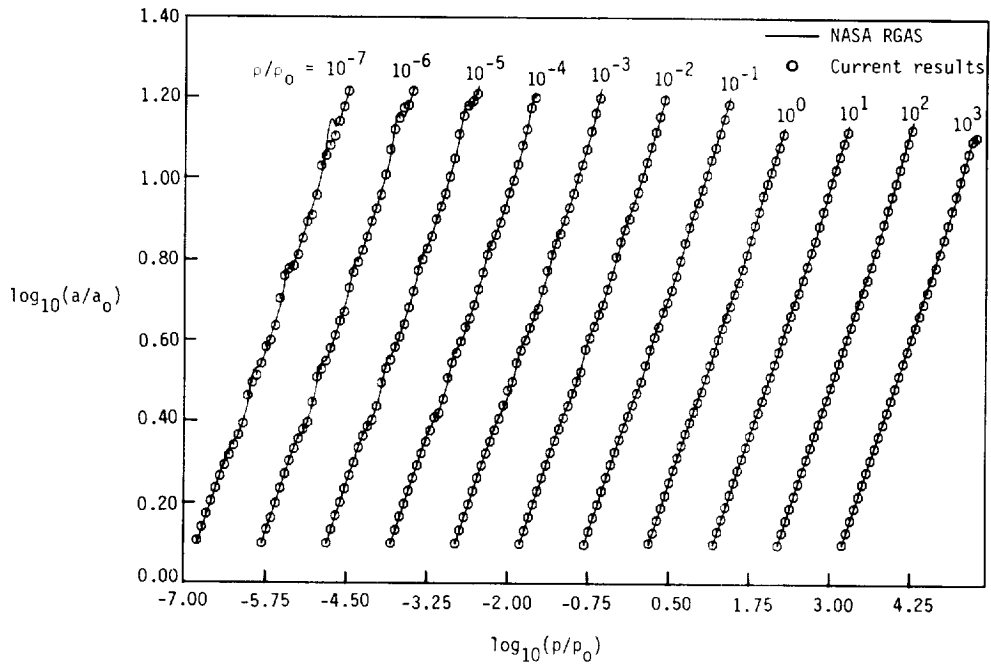


Figure 19. Comparison of curve fits for  $a = a(p, s)$ .

very difficult to maintain continuity at the juncture points. This was due to the manner in which the domain was subdivided to obtain the piecewise approximating functions. However, discontinuities were kept to a minimum, with average mismatches of 2.4 percent for  $\rho = \rho(p, s)$ , 1.2 percent for  $a = a(p, s)$ , and 2.0 percent for  $e = e(p, s)$ .

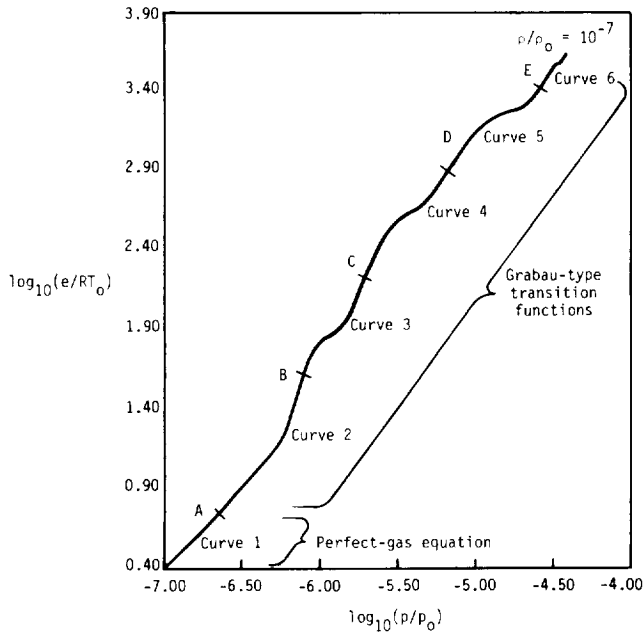


Figure 20. Example curve fit for  $p = p(e, \rho)$ .

A comparison of the relative computer times required for the new curve fit subroutines and the NASA RGAS program on the National Advanced Systems 9160 computer is given in table 15. The new subroutine for determining  $p = p(e, \rho)$ ,  $a = a(e, \rho)$ , and  $T = T(e, \rho)$  was 2.4 times faster than the NASA RGAS subroutine. The previous subroutine (ref. 15) for the same curve fits was 3.4 times faster than the NASA RGAS subroutine. The new

subroutine for  $T = T(p, \rho)$  was 2.7 times faster than the NASA RGAS subroutine, and the previous subroutine (ref. 15) was 3.4 times faster. The new subroutine for  $h = h(p, \rho)$  was 3.2 times faster than the NASA RGAS subroutine, compared with the previous subroutine (ref. 15), which was 4.4 times faster. The subroutine for  $s = s(e, \rho)$  was 10.2 times faster than the NASA RGAS program. The new subroutines for the curve fits  $\rho = \rho(p, s)$ ,  $e = e(p, s)$ , and  $a = a(p, s)$  were approximately 10 times faster than the NASA RGAS subroutine. It should be noted that the NASA RGAS program requires two data files for storage of the cubic interpolation coefficients. The fact that these data files are now on disk and not tape has significantly speeded up the NASA RGAS subroutine. However, the curve fits still provide a substantial improvement in computing time, being 2.4 to 10.2 times faster than the table-lookup technique.

In conclusion, the new, simplified curve fits for the thermodynamic properties of equilibrium air provide substantial reductions in computer time and storage while maintaining good accuracy. They can be incorporated into computational fluid dynamics computer codes in a straightforward manner without the need for data files. The improved accuracy of the new curve fits permits their use in time-dependent flow calculations from start-up to the final steady-state solution. In addition, the improved continuity of these curve fits permits their use in iterative calculations. For example, the new curve fit for  $h = h(p, \rho)$  can be employed in the iterative procedure required to "fit" a bow shock in equilibrium flow. However, the discontinuities which still exist in the entropy curve fits may cause difficulties when used in an iterative shock calculation.

NASA Langley Research Center  
Hampton, Virginia 23665-5225  
May 1, 1987

Table 1. Accuracy of  $p = p(e, \rho)$

Total number of data points = 22 239

Current results: Maximum error = 3.93 percent

$$\log_{10}(\rho/\rho_0) = 4.0; \log_{10}(e/RT_0) = 3.28$$

$$T = 1.47 \times 10^4 \text{K}$$

Ref. 15 results: Maximum error = 9.00 percent

$$\log_{10}(\rho/\rho_0) = -4.5; \log_{10}(e/RT_0) = 2.236$$

$$T = 4.53 \times 10^3 \text{K}$$

Error, percent	Current results, percent	Results from ref. 15, percent
0.5	28.43	68.29
1.0	10.63	42.87
2.0	1.01	17.51
3.0	.03	6.69
4.0	0	1.49
5.0	0	.24
6.0	0	.14
7.0	0	.04
8.0	0	.01
9.0	0	0
$\geq 10.0$	0	0

Table 2. Accuracy of  $a = a(e, \rho)$

Total number of data points = 22 239

Current results: Maximum error = 4.48 percent

$$\log_{10}(\rho/\rho_0) = -3.0; \log_{10}(e/RT_0) = 3.318$$

$$T = 2.0 \times 10^4 \text{K}$$

Ref. 15 results: Maximum error = 4.94 percent

$$\log_{10}(\rho/\rho_0) = -7.0; \log_{10}(e/RT_0) = 3.279$$

$$T = 1.25 \times 10^4 \text{K}$$

Error, percent	Current results, percent	Results from ref. 15, percent
0.5	20.94	60.67
1.0	5.75	27.21
2.0	.70	5.17
3.0	.09	.98
4.0	.02	.11
5.0	0	0
6.0	0	0
7.0	0	0
8.0	0	0
9.0	0	0
$\geq 10.0$	0	0



Table 3. Accuracy of  $T = T(e, \rho)$

Total number of data points = 22 239

Current results: Maximum error = 4.36 percent

$$\log_{10}(\rho/\rho_0) = -4.0; \log_{10}(e/RT_0) = 3.28$$

$$T = 1.47 \times 10^4 \text{K}$$

Ref. 15 results: Maximum error = 8.8 percent

$$\log_{10}(\rho/\rho_0) = -0.625; \log_{10}(e/RT_0) = 3.255$$

$$T = 2.4 \times 10^4 \text{K}$$

Error, percent	Current results, percent	Results from ref. 15, percent
0.5	34.11	63.82
1.0	10.87	34.74
2.0	.58	9.51
3.0	.10	2.43
4.0	.01	.59
5.0	0	.19
6.0	0	.09
7.0	0	.04
8.0	0	.02
9.0	0	0
$\geq 10.0$	0	0

Table 4. Accuracy of  $s = s(e, \rho)$

Total number of data points = 21 975

Current results: Maximum error = 2.51 percent

$$\log_{10}(\rho/\rho_0) = -0.625; \log_{10}(e/RT_0) = 0.657$$

$$T = 4.89 \times 10^2 \text{K}$$

Error, percent	Current results, percent
0.5	49.77
1.0	15.95
2.0	.56
3.0	0
4.0	0
5.0	0
6.0	0
7.0	0
8.0	0
9.0	0
$\geq 10.0$	0

Table 5. Accuracy of  $T = T(p, \rho)$

Total number of data points = 22 239

Current results: Maximum error = 3.9 percent

$$\log_{10}(\rho/\rho_0) = -3.25; \log_{10}(p/p_0) - \log_{10}(\rho/\rho_0) = 2.58$$

$$T = 2.4 \times 10^4 \text{K}$$

Ref. 15 results: Maximum error = 5.71 percent

$$\log_{10}(\rho/\rho_0) = -0.625; \log_{10}(p/p_0) - \log_{10}(\rho/\rho_0) = 2.44$$

$$T = 2.3 \times 10^4 \text{K}$$

Error, percent	Current results, percent	Results from ref. 15, percent
0.5	22.89	58.82
1.0	8.24	28.75
2.0	.22	4.89
3.0	.03	.96
4.0	0	.16
5.0	0	.04
6.0	0	0
7.0	0	0
8.0	0	0
9.0	0	0
$\geq 10.0$	0	0

Table 6. Accuracy of  $h = h(p, \rho)$

Total number of data points = 22 239

Current results: Maximum error = 3.44 percent

$$\log_{10}(\rho/\rho_0) = -7.0; \log_{10}(p/p_0) - \log_{10}(\rho/\rho_0) = 2.60$$

$$T = 1.91 \times 10^4 \text{K}$$

Ref. 15 results: Maximum error = 6.56 percent

$$\log_{10}(\rho/\rho_0) = -4.5; \log_{10}(p/p_0) - \log_{10}(\rho/\rho_0) = 1.01$$

$$T = 2.47 \times 10^3 \text{K}$$

Error, percent	Current results, percent	Results from ref. 15, percent
0.5	23.85	67.45
1.0	7.65	40.36
2.0	.55	13.65
3.0	.04	4.78
4.0	0	1.56
5.0	0	.46
6.0	0	.16
7.0	0	0
8.0	0	0
9.0	0	0
$\geq 10.0$	0	0

Table 7. Accuracy of  $\rho = \rho(p, s)$

Total number of data points = 21 030

Current results: Maximum error = 7.58 percent

$$\log_{10}(\rho/\rho_0) = -6.625; \log_{10}(e/RT_0) = 3.30$$

$$T = 1.42 \times 10^4 \text{K}$$

Error, percent	Current results, percent
0.5	62.06
1.0	40.25
2.0	14.97
3.0	4.46
4.0	.98
5.0	.35
6.0	.03
7.0	.01
8.0	0
9.0	0
$\geq 10.0$	0

Table 8. Accuracy of  $e = e(p, s)$

Total number of data points = 21 030

Current results: Maximum error = 4.5 percent

$$\log_{10}(\rho/\rho_0) = 2.875; \log_{10}(e/RT_0) = 2.85$$

$$T = 2.46 \times 10^4 \text{K}$$

Error, percent	Current results, percent
0.5	39.52
1.0	22.68
2.0	5.45
3.0	.04
4.0	.01
5.0	0
6.0	0
7.0	0
8.0	0
9.0	0
$\geq 10.0$	0

Table 9. Accuracy of  $a = a(p, s)$

Total number of data points = 21 030

Current results: Maximum error = 6.1 percent

$$\log_{10}(\rho/\rho_0) = -2.375; \log_{10}(e/RT_0) = 2.39$$

$$T = 6.05 \times 10^3 \text{K}$$

Error, percent	Current results, percent
0.5	50.98
1.0	26.28
2.0	5.74
3.0	1.67
4.0	.48
5.0	.08
6.0	0
7.0	0
8.0	0
9.0	0
$\geq 10.0$	0

Table 10. Comparison of Variables at Juncture Points for  $p = p(\epsilon, \rho)$

Density ratio, $\rho/\rho_0$	Point A*		Point B*		Point C*		Point D*		Point E*	
	Lower	Upper	Lower	Upper	Lower	Upper	Lower	Upper	Lower	Upper
$10^{-7}$	$1.79 \times 10^{-2}$	$1.81 \times 10^{-2}$	$7.32 \times 10^{-2}$	$7.38 \times 10^{-2}$	$1.90 \times 10^{-1}$	$1.90 \times 10^{-1}$	$8.72 \times 10^{-1}$	$8.72 \times 10^{-1}$	$2.62 \times 10^0$	$2.63 \times 10^0$
$10^{-6}$	$1.79 \times 10^{-1}$	$1.80 \times 10^{-1}$	$7.81 \times 10^{-1}$	$7.78 \times 10^{-1}$	$2.01 \times 10^0$	$2.03 \times 10^0$	$9.53 \times 10^0$	$9.63 \times 10^0$	$2.86 \times 10^1$	$2.89 \times 10^1$
$10^{-5}$	$1.79 \times 10^0$	$1.80 \times 10^0$	$8.17 \times 10^0$	$8.19 \times 10^0$	$2.16 \times 10^1$	$2.18 \times 10^1$	$1.05 \times 10^2$	$1.06 \times 10^2$	$3.15 \times 10^2$	$3.16 \times 10^2$
$10^{-4}$	$1.80 \times 10^1$	$1.81 \times 10^1$	$8.67 \times 10^1$	$8.70 \times 10^1$	$2.40 \times 10^2$	$2.43 \times 10^2$	$9.78 \times 10^2$	$9.79 \times 10^2$	$1.80 \times 10^2$	$1.81 \times 10^2$
$10^{-3}$	$1.80 \times 10^2$	$1.81 \times 10^2$	$9.12 \times 10^2$	$9.13 \times 10^2$	$2.61 \times 10^3$	$2.63 \times 10^3$	$1.09 \times 10^4$	$1.09 \times 10^4$		
$10^{-2}$	$1.80 \times 10^3$	$1.81 \times 10^3$	$9.51 \times 10^3$	$9.51 \times 10^3$	$2.83 \times 10^4$	$2.84 \times 10^4$	$1.23 \times 10^5$	$1.23 \times 10^5$		
$10^{-1}$	$1.80 \times 10^4$	$1.81 \times 10^4$	$9.80 \times 10^4$	$9.81 \times 10^4$	$3.08 \times 10^5$	$3.08 \times 10^5$	$1.39 \times 10^6$	$1.39 \times 10^6$		
$10^0$	$1.80 \times 10^5$	$1.81 \times 10^5$	$1.36 \times 10^6$	$1.36 \times 10^6$	$4.11 \times 10^6$	$4.11 \times 10^6$				
$10^1$	$1.80 \times 10^6$	$1.81 \times 10^6$	$1.41 \times 10^7$	$1.41 \times 10^7$	$4.50 \times 10^7$	$4.54 \times 10^7$				
$10^2$	$1.80 \times 10^7$	$1.81 \times 10^7$	$1.45 \times 10^8$	$1.43 \times 10^8$	$4.91 \times 10^8$	$5.00 \times 10^8$				
$10^3$	$1.80 \times 10^8$	$1.83 \times 10^8$	$1.48 \times 10^9$	$1.45 \times 10^9$	$5.42 \times 10^9$	$5.53 \times 10^9$				

\*See figure 20 for curve breaks.

Table 11. Comparison of Variables at Juncture Points for  $a = a(\epsilon, \rho)$

Density ratio, $\rho/\rho_0$	Point A*		Point B*		Point C*		Point D*		Point E*	
	Lower	Upper	Lower	Upper	Lower	Upper	Lower	Upper	Lower	Upper
$10^{-7}$	440	441	769	790	1250	1260	2718	2733	4731	4715
$10^{-6}$	440	439	808	814	1291	1307	2857	2871	4983	5016
$10^{-5}$	440	438	831	841	1343	1359	3021	3029	5259	5287
$10^{-4}$	441	440	869	874	1429	1441	2923	2925		
$10^{-3}$	441	440	902	904	1498	1506	3115	3116		
$10^{-2}$	441	440	932	932	1573	1578	3337	3341		
$10^{-1}$	441	441	957	957	1655	1656	3596	3602		
$10^0$	442	441	1120	1118	1924	1924				
$10^1$	442	440	1149	1145	2027	2039				
$10^2$	442	440	1171	1164	2141	2166				
$10^3$	442	441	1188	1179	2287	2312				

\*See figure 20 for curve breaks.

Table 12. Comparison of Variables at Juncture Points for  $T = T(\epsilon, \rho)$

Density ratio, $\rho/\rho_0$	Point A*		Point B*		Point C*		Point D*		Point E*	
	Lower	Upper	Lower	Upper	Lower	Upper	Lower	Upper	Lower	Upper
$10^{-7}$	486	481	2112	2091	4033	4034	7868	7869		
$10^{-6}$	486	482	2181	2168	4283	4284	8471	8479		
$10^{-5}$	486	484	2243	2243	4548	4548	9145	9146		
$10^{-4}$	486	481	2312	2312	4837	4818	10364	10319		
$10^{-3}$	486	481	2347	2366	5090	5088	11190	11177		
$10^{-2}$	486	481	2376	2404	5307	5326	11958	12006		
$10^{-1}$	486	481	2400	2417	5508	5517	12702	12738		
$10^0$	486	482	2408	2414	6242	6265				
$10^1$	486	482	2413	2416	6585	6595				
$10^2$	486	482	2416	2416	6955	6960				
$10^3$	486	483	2418	2419	7317	7328				

\*See figure 20 for curve breaks.

Table 13. Comparison of Variables at Juncture Points for  $T = T(p, \rho)$

Density ratio, $\rho/\rho_0$	Point A*		Point B*		Point C*		Point D*		Point E*	
	Lower	Upper	Lower	Upper	Lower	Upper	Lower	Upper	Lower	Upper
$10^{-7}$	486	482	2089	2089	4025	4033	7864	7838		
$10^{-6}$	486	482	2165	2165	4281	4281	8470	8481		
$10^{-5}$	486	484	2242	2242	4549	4554	9146	9146		
$10^{-4}$	486	482	2310	2310	5064	5042	10796	10746		
$10^{-3}$	486	481	2363	2363	5386	5376	11793	11682		
$10^{-2}$	486	481	2404	2404	5690	5701	12742	12679		
$10^{-1}$	486	482	2402	2402	5968	5998	13671	13687		
$10^0$	486	482	2700	2700	6248	6267				
$10^1$	486	482	2706	2710	6585	6598				
$10^2$	486	483	2711	2712	6950	6959				
$10^3$	486	483	2713	2713	7309	7319				

\*See figure 20 for curve breaks.

Table 14. Comparison of Variables at Juncture Points for  $h = h(p, \rho)$

Density ratio, $\rho/\rho_0$	Point A*		Point B*		Point C*		Point D*		Point E*	
	Lower	Upper	Lower	Upper	Lower	Upper	Lower	Upper	Lower	Upper
$10^{-7}$	$0.346 \times 10^6$	$0.346 \times 10^6$	$0.282 \times 10^7$	$0.285 \times 10^7$	$0.160 \times 10^8$	$0.159 \times 10^8$	$0.997 \times 10^8$	$0.997 \times 10^8$		
$10^{-6}$	.346	.346	.253	.254	.138	.138	.890	.890		
$10^{-5}$	.346	.346	.233	.235	.120	.122	.793	.792		
$10^{-4}$	.346	.346	.345	.345	.247	.247	.812	.813		
$10^{-3}$	.346	.346	.314	.315	.214	.214	.720	.721		
$10^{-2}$	.346	.346	.296	.296	.186	.186	.646	.646		
$10^{-1}$	.346	.346	.288	.288	.164	.164	.590	.591		
$10^0$	.345	.345	.386	.387	.201	.202				
$10^1$	.345	.345	.377	.380	.180	.181				
$10^2$	.345	.345	.374	.376	.166	.166				
$10^3$	.345	.345	.374	.374	.156	.156				

\*See figure 20 for curve breaks.

Table 15. Comparison of Computer Times

Curve fit	Number of data points	Computer time, s, for		
		Old subroutine (ref. 15)	New subroutine	NASA RGAS
$p = p(e, \rho)$ $a = a(e, \rho)$ $T = T(e, \rho)$	10661	0.54	0.77	1.86
$s = s(e, \rho)$	10661		.20	2.03
$T = T(p, \rho)$	9921	.25	.31	.84
$h = h(p, \rho)$	9921	.19	.26	.84
$\rho = \rho(p, s)$	3038		.10	1.07
$e = e(p, s)$	3038		.11	1.06
$a = a(p, s)$	3038		.11	1.06

## Appendix A

### Curve Fit Coefficients

$$\mathbf{p} = \mathbf{p}(e, \rho)$$

The coefficients  $a_1, a_2, \dots, a_{24}$  and the proper sign before the exponential term of the Grabau transition in equation (26) are given in tables A1 to A3. Table A1 is for the density range  $-7.0 \leq Y \leq -4.5$ , table A2 is for  $-4.5 < Y \leq -0.5$ , and table A3 is for  $-0.5 < Y \leq 3.0$ , where  $Y = \log_{10}(\rho/\rho_0)$ .

The following linear interpolation technique was adopted for all the curve fits where density was one of the independent variables. In general, for  $f = f(Y, Z)$ , where  $f$  is the dependent variable,  $Y = \log_{10}(\rho/\rho_0)$ , and  $Z$  is the second independent variable (either internal energy or pressure), if  $|Y - (-4.5)| < 2.5 \times 10^{-2}$ , then

$$f(Y, Z) = f(-4.475, Z) + [f(-4.475, Z) - f(-4.525, Z)] \times (Y + 4.525)/0.05 \quad (\text{A1})$$

If  $|Y - (-0.5)| < 5.0 \times 10^{-3}$ , then

$$f(Y, Z) = f(-0.495, Z) + [f(-0.495, Z) - f(-0.505, Z)] \times (Y + 0.505)/0.01 \quad (\text{A2})$$

$$\mathbf{a} = \mathbf{a}(e, \rho)$$

The exact expression for  $a$  was given in equation (27). The expressions for  $\left(\frac{\partial \tilde{\gamma}}{\partial \ln e}\right)_\rho$  and  $\left(\frac{\partial \tilde{\gamma}}{\partial \ln \rho}\right)_e$  are given below:

$$\left(\frac{\partial \tilde{\gamma}}{\partial \ln \rho}\right)_e = \frac{1}{\ln 10} \frac{\partial \tilde{\gamma}}{\partial \gamma} \quad (\text{A3})$$

where

$$\begin{aligned} \frac{\partial \tilde{\gamma}}{\partial Y} = & a_2 + a_4 Z + 2a_5 Y + 2a_7 Y Z + a_8 Z^2 + 3a_9 Y^2 \\ & + (a_{12} + a_{14} Z + 2a_{15} Y + 2a_{17} Y Z + a_{18} Z^2 + 3a_{19} Y^2)/ \\ & [1 \pm \exp(a_{21} + a_{22} Y + a_{23} Z + a_{24} Y Z)] \\ & \mp (a_{11} + a_{12} Y + a_{13} Z + a_{14} Y Z + a_{15} Y^2 + a_{16} Z^2 \\ & + a_{17} Y^2 Z + a_{18} Y Z^2 + a_{19} Y^3 + a_{20} Z^3)(a_{22} + a_{24} Z) \\ & [\exp(a_{21} + a_{22} Y + a_{23} Z + a_{24} Y Z)/ \\ & [1 \pm \exp(a_{21} + a_{22} Y + a_{23} Z + a_{24} Y Z)]]^2 \end{aligned} \quad (\text{A4})$$

$$\left(\frac{\partial \tilde{\gamma}}{\partial \ln e}\right)_\rho = \frac{1}{\ln 10} \frac{\partial \tilde{\gamma}}{\partial Z} \quad (\text{A5})$$

where

$$\begin{aligned} \frac{\partial \tilde{\gamma}}{\partial Z} = & a_3 + a_4 Y + 2a_6 Z + a_7 Y^2 + 2a_8 Y Z + 3a_{10} Z^2 \\ & + (a_{13} + a_{14} Y - 2a_{16} Z + 2a_{17} Y^2 + 2a_{18} Y Z \\ & + 3a_{20} Z^2)/[1 \pm \exp(a_{21} + a_{22} Y \\ & + a_{23} Z + a_{24} Y Z)] \mp (a_{11} + a_{12} Y + a_{13} Z \\ & + a_{14} Y Z + a_{15} Y^2 + a_{16} Z^2 + a_{17} Y^2 Z \\ & + a_{18} Y Z^2 + a_{19} Y^3 + a_{20} Z^3)(a_{23} + a_{24} Y) \\ & [\exp(a_{21} + a_{22} Y + a_{23} Z + a_{24} Y Z)]/ \\ & [1 \pm \exp(a_{21} + a_{22} Y + a_{23} Z + a_{24} Y Z)]^2 \end{aligned} \quad (\text{A6})$$

The coefficients  $a_1, a_2, \dots, a_{24}$  are presented in tables A1 to A3.

$$\mathbf{T} = \mathbf{T}(e, \rho)$$

Coefficients  $b_1, b_2, \dots, b_{24}$  are presented in tables A4, A5, and A6, where equation (28) gives the form of the curve fit.

$$\mathbf{h} = \mathbf{h}(\mathbf{p}, \rho)$$

The equation of the curve fit is given by equation (30). The coefficients  $c_1, c_2, \dots, c_{24}$  and the sign before the exponent of the Grabau transition function are presented in tables A7, A8, and A9.

$$\mathbf{T} = \mathbf{T}(\mathbf{p}, \rho)$$

The coefficients  $d_1, d_2, \dots, d_{24}$  of the curve fit, equation (31), are presented in tables A10, A11, and A12.

$$\mathbf{s} = \mathbf{s}(e, \rho)$$

The coefficients  $e_1, e_2, \dots, e_{10}$  of the curve fit, equation (32), are presented in table A13.

$$\rho = \rho(\mathbf{p}, \mathbf{s})$$

The general form of the curve fit is given by equation (33). The coefficients  $f_1, f_2, \dots, f_{25}$  are presented in table A14.

$$\mathbf{e} = \mathbf{e}(\mathbf{p}, \mathbf{s})$$

The coefficients  $g_1, g_2, \dots, g_{25}$  of the curve fit, equation (34), are presented in table A15.

$$\mathbf{a} = \mathbf{a}(\mathbf{p}, \mathbf{s})$$

The curve fit is given by equation (35). The coefficients  $h_1, h_2, \dots, h_{25}$  are presented in table A16.



Table A1. Coefficients for  $p = p(e, \rho)$  and  $a = a(e, \rho)$  for  $-7.0 \leq Y \leq -4.5$

Coefficient	Values for range of $Z$ of --							
	$Z \leq 0.65$	$0.65 < Z \leq 1.50$	$1.50 < Z \leq 2.20$	$2.20 < Z \leq 3.05$	$3.05 < Z \leq 3.40$	$3.40 < Z$		
$a_1$	1.3965E00	1.52792E00	-1.70333E01	2.24374E00	-0.20807E02	-5.22951E01		
$a_2$	0	-1.26953E-02	-5.08545E-01	1.03073E-01	.40197E00	-4.00011E-01		
$a_3$	0	-6.13514E-01	2.46299E01	-5.32238E-01	.22591E02	4.56439E01		
$a_4$	0	-5.08262E-02	4.45617E-01	-5.59852E-02	- .25660E00	2.24484E-01		
$a_5$	0	-5.49384E-03	-8.95298E-03	3.56484E-03	- .95833E-03	-3.73775E-03		
$a_6$	0	6.31835E-01	-1.10204E01	-4.80156E-02	- .77174E01	-1.29756E01		
$a_7$	0	4.75120E-05	2.29618E-03	-1.01359E-04	.23966E-02	2.43161E-03		
$a_8$	0	3.34012E-02	-9.89727E-02	1.06794E-02	.4606E-01	-2.79517E-02		
$a_9$	0	-3.18468E-04	-2.89186E-04	1.59127E-04	.33671E-03	2.24755E-04		
$a_{10}$	0	-2.19921E-01	1.62903E00	3.66035E-02	.878E00	1.22998E00		
$a_{11}$	0	-4.96286E01	1.86797E01	-5.70378E00	- .21737E03	0		
$a_{12}$	0	-1.17932E01	5.19662E-01	-3.10056E-01	- .46927E01	0		
$a_{13}$	0	6.91028E01	-2.41338E01	5.01094E00	.18101E03	0		
$a_{14}$	0	4.40405E01	-4.34837E-01	1.80411E-01	.26621E01	0		
$a_{15}$	0	5.09249E00	9.16089E-03	-9.49361E-03	- .34759E-01	0		
$a_{16}$	0	1.37308E01	1.02035E01	-1.40331E00	- .50019E02	0		
$a_{17}$	0	-1.40326E00	-1.52082E-03	1.94839E-03	.64681E-02	0		
$a_{18}$	0	-1.78726E01	9.70762E-02	-2.79718E-02	- .38381E00	0		
$a_{19}$	0	2.08988E-01	3.46482E-04	-2.24908E-04	- .70391E-03	0		
$a_{20}$	0	-1.86943E01	-1.3946E00	1.20278E-01	.45795E01	0		
$a_{21}$	0	24.60452E00	-1.42762E02	1.139755E02	.4544373E03	0		
$a_{22}$	0	-2.0E00	-1.647088E00	-4.985467E00	.1250133E02	0		
$a_{23}$	0	-2.093022E01	7.660312E01	-4.223833E01	- .1376001E03	0		
$a_{24}$	0	0	8.259346E-01	2.009706E00	- .3641774E01	0		
Sign	+	-	+	+	+	+		

Table A2. Coefficients for  $p = p(e, \rho)$  and  $a = a(e, \rho)$  for  $-4.5 < Y \leq -0.5$

Coefficient	Values for range of $Z$ of —					
	$Z \leq 0.65$	$0.65 < Z \leq 1.50$	$1.50 < Z \leq 2.22$	$2.22 < Z \leq 2.95$	$2.95 < Z$	
$a_1$	1.398E00	1.39123E00	-1.20784E00	-2.26460E00	-1.66904E01	
$a_2$	0	-4.08321E-03	-2.57909E-01	-7.82263E-02	-2.58318E-01	
$a_3$	0	1.42545E-02	5.02307E00	4.90497E00	1.78350E01	
$a_4$	0	1.41769E-02	2.87201E-01	7.18096E-02	1.54898E-01	
$a_5$	0	2.57225E-04	-9.95577E-03	-3.06443E-03	-9.71263E-03	
$a_6$	0	6.2555E-02	-3.20619E00	-2.24750E00	-5.94108E00	
$a_7$	0	6.52912E-04	5.23524E-03	1.74209E-03	3.97740E-03	
$a_8$	0	-7.83637E-03	-7.50405E-02	-1.31641E-02	-2.01335E-02	
$a_9$	0	8.46912E-05	-1.45574E-04	2.84214E-05	9.04300E-05	
$a_{10}$	0	-9.78720E-02	6.51564E-01	3.33658E-01	6.60432E-01	
$a_{11}$	0	5.80955E00	-6.62841E00	-1.47904E01	8.54690E01	
$a_{12}$	0	-1.82302E-01	2.77112E-02	-1.76627E-01	1.17554E01	
$a_{13}$	0	-9.62396E00	7.30762E00	1.35036E01	-7.21760E01	
$a_{14}$	0	1.79619E-01	-7.6823E-02	8.77280E-02	-7.15723E00	
$a_{15}$	0	-2.30518E-02	7.19421E-03	-2.13327E-03	-4.16150E-02	
$a_{16}$	0	5.27047E00	-2.33161E00	-3.95372E00	2.01758E01	
$a_{17}$	0	1.1872E-02	-3.62463E-03	7.15487E-04	1.38147E-02	
$a_{18}$	0	-3.65507E-02	3.04767E-02	-8.96151E-03	1.08990E00	
$a_{19}$	0	-3.35499E-04	1.62777E-04	7.30928E-05	5.45184E-04	
$a_{20}$	0	-9.19897E-01	1.66856E-01	3.63229E-01	-1.86438E00	
$a_{21}$	0	14.2E00	1.255324E02	1.788542E02	2.883262E02	
$a_{22}$	0	0	2.015335E00	6.317894E00	1.248536E01	
$a_{23}$	0	-1.00E01	-6.390747E01	-6.756741E01	-8.816985E01	
$a_{24}$	0	0	-6.515225E-01	-2.46006E00	-3.720309E00	
Sign	+	+	+	+	+	

Table A3. Coefficients for  $p = p(e, \rho)$  and  $a = a(e, \rho)$  for  $-0.5 < Y \leq 3.0$

Coefficient	Values for range of $Z$ of				
	$Z \leq 0.65$	$0.65 < Z \leq 1.70$	$1.70 < Z \leq 2.35$	$2.35 < Z$	
$a_1$	1.3988E00	1.37062E00	3.43846E-02	-1.70633E00	
$a_2$	0	1.29673E-02	-2.33584E-01	-1.48403E-01	
$a_3$	0	1.11418E-01	2.85574E00	4.23104E00	
$a_4$	0	-3.26912E-02	2.59787E-01	1.37290E-01	
$a_5$	0	1.06869E-03	-10.89927E-03	-9.10934E-03	
$a_6$	0	-1.06133E-01	-1.94785E00	-1.97292E00	
$a_7$	0	-2.00286E-03	4.23659E-03	3.85707E-03	
$a_8$	0	1.90251E-02	-6.73865E-02	-2.81830E-02	
$a_9$	0	2.38305E-04	3.85712E-04	2.69026E-04	
$a_{10}$	0	3.02210E-03	4.08518E-01	2.95882E-01	
$a_{11}$	0	0	-4.20569E00	3.41580E01	
$a_{12}$	0	0	1.33139E-01	-1.89972E01	
$a_{13}$	0	0	4.51236E00	-4.0858E01	
$a_{14}$	0	0	-1.66341E-01	1.30321E01	
$a_{15}$	0	0	1.67787E-03	-8.01272E-01	
$a_{16}$	0	0	-1.35516E00	1.60826E01	
$a_{17}$	0	0	-1.10022E-03	2.75121E-01	
$a_{18}$	0	0	4.91716E-02	-2.23386E00	
$a_{19}$	0	0	3.06676E-04	-1.77969E-04	
$a_{20}$	0	0	7.52509E-02	-2.08853E00	
$a_{21}$	0	0	1.757042E02	2.561323E02	
$a_{22}$	0	0	-2.163278E00	1.737089E02	
$a_{23}$	0	0	-8.833702E01	-9.05889E01	
$a_{24}$	0	0	1.897543E00	-5.838803E01	
Sign	+	+	+	+	+

Table A4. Coefficients for  $T = T(e, \rho)$  for  $-7.0 \leq Y \leq -4.5$ 

Coefficient	Values <sup>a</sup> for range of $Z$ of ...			
	$0.25 < Z \leq 0.95$	$0.95 < Z \leq 1.40$	$1.40 < Z \leq 1.95$	$1.95 < Z$
$b_1$	1.44824E-01	-9.325E00	-1.93082E01	-2.59721E01
$b_2$	1.36744E-02	-9.32017E-01	-1.54557E00	-1.77419E00
$b_3$	1.17099E-01	2.57176E01	3.69035E01	3.62495E01
$b_4$	-8.22299E-02	1.61292E00	1.92214E00	1.55383E00
$b_5$	-6.75303E-04	-3.00242E-02	-3.59027E-02	-4.51359E-02
$b_6$	1.3937E00	-2.1662E01	-2.20440E01	-1.59988E01
$b_7$	-1.47314E-03	2.62959E-02	2.31827E-02	2.43648E-02
$b_8$	6.83066E-02	-6.81431E-01	-5.80935E-01	-3.17807E-01
$b_9$	-7.90851E-05	-2.77651E-04	-2.01327E-04	1.2804E-04
$b_{10}$	-6.65673E-01	6.26962E00	4.43367E00	2.40584E00
$b_{11}$	0	-3.38534E00	-3.83069E00	-1.81433E01
$b_{12}$	0	1.82594E-01	1.32864E-01	1.54896E-01
$b_{13}$	0	1.84928E-01	-3.91902E00	1.26582E01
$b_{14}$	0	-7.01109E-01	-6.79564E-01	-3.66275E-01
$b_{15}$	0	1.10150E-02	6.06341E-04	3.24496E-02
$b_{16}$	0	5.4702E00	7.24632E00	-1.41759E00
$b_{17}$	0	-1.60570E-02	-8.12997E-03	-1.66385E-02
$b_{18}$	0	4.11624E-01	3.15461E-01	1.11241E-01
$b_{19}$	0	1.57701E-05	-1.61012E-04	3.02177E-04
$b_{20}$	0	-2.81498E00	-2.17879E00	-3.10983E-01
$b_{21}$	0	-3.887015E01	2.08E01	1.115884E02
$b_{22}$	0	-2.908228E01	-2.56E01	-6.452606E00
$b_{23}$	0	4.070557E01	1.0E00	-5.337863E01
$b_{24}$	0	2.682347E01	1.80E01	2.026986E00

<sup>a</sup> For  $Z \leq 0.25$ ,  $T = p(e, \rho)/\rho R$ .

Table A5. Coefficients for  $T = T(e, \rho)$  for  $-4.5 < Y \leq -0.5$ .

Coefficient	Values <sup>a</sup> for range of $Z$ of —			
	$0.25 < Z \leq 0.95$	$0.95 < Z \leq 1.40$	$1.40 < Z \leq 2.00$	$2.00 < Z$
$b_1$	2.94996E-02	-5.53324E00	-1.13598E01	-1.76079E01
$b_2$	7.24997E-03	-3.53749E-01	-1.02049E00	-1.26579E00
$b_3$	7.81783E-01	1.63638E01	2.22793E01	2.48544E01
$b_4$	-3.27402E-01	5.87547E-01	1.24038E00	1.09442E00
$b_5$	3.23357E-04	-1.16081E-02	-3.10771E-02	-3.65534E-02
$b_6$	3.95198E-01	-1.41239E01	-1.31512E01	-1.08166E01
$b_7$	-9.69989E-04	7.99571E-03	1.92551E-02	1.54346E-02
$b_8$	2.92926E-02	-2.35146E-01	-3.62875E-01	-2.27803E-01
$b_9$	-8.9324E-06	-2.79316E-04	-2.69140E-04	-4.59822E-04
$b_{10}$	-2.12182E-01	4.28891E00	2.64544E00	1.60641E00
$b_{11}$	0	9.07979E00	8.72852E00	2.60669E01
$b_{12}$	0	1.01308E00	1.27564E00	2.31791E00
$b_{13}$	0	-2.29428E01	-1.79172E01	-3.22433E01
$b_{14}$	0	-1.52122E00	-1.52051E00	-1.82645E00
$b_{15}$	0	3.78390E-02	4.91264E-02	4.94621E-02
$b_{16}$	0	1.95657E01	1.16719E01	1.33829E01
$b_{17}$	0	-2.63115E-02	-2.81731E-02	-1.85542E-02
$b_{18}$	0	5.73839E-01	4.5413E-01	3.59744E-01
$b_{19}$	0	5.46402E-04	5.23383E-04	5.04815E-04
$b_{20}$	0	-5.63057E00	-2.45584E00	-1.86517E00
$b_{21}$	0	7.619803E01	1.84792E02	3.093755E02
$b_{22}$	0	-1.501155E01	9.583443E00	1.875018E01
$b_{23}$	0	-6.770845E01	-1.020835E02	-1.375004E02
$b_{24}$	0	1.273147E01	-4.166727E00	-8.333418E00

<sup>a</sup> For  $Z \leq 0.25$ ,  $T = p(e, \rho)/\rho R$ .

Table A6. Coefficients for  $T = T(e, \rho)$  for  $-0.5 < Y \leq 3.0$ 

Coefficient	Values <sup>a</sup> for range of $Z$ of -		
	$0.25 < Z \leq 0.95$	$0.95 < Z \leq 1.45$	$1.45 < Z$
$b_1$	-2.94081E-03	1.32396E00	-1.60643E00
$b_2$	5.73915E-04	8.52771E-02	-5.07368E-02
$b_3$	9.88883E-01	-3.24257E00	3.95872E00
$b_4$	-3.71241E-03	-2.00937E-01	3.69383E-02
$b_5$	1.12387E-04	5.68146E-03	-1.59378E-03
$b_6$	2.86656E-02	4.53823E00	-1.71201E00
$b_7$	-3.76528E-04	-6.85856E-03	1.06057E-03
$b_8$	4.56059E-03	1.18123E-01	9.25124E-03
$b_9$	1.76192E-05	1.98366E-04	6.53278E-05
$b_{10}$	-1.99498E-02	-1.6246E00	2.71039E-01
$b_{11}$	0	-5.26673E-01	1.80476E01
$b_{12}$	0	-1.58691E-01	1.62964E00
$b_{13}$	0	2.61600E00	-2.73124E01
$b_{14}$	0	3.16356E-01	-1.57430E00
$b_{15}$	0	-1.90755E-02	5.85277E-02
$b_{16}$	0	-3.3793E00	1.36342E01
$b_{17}$	0	1.70124E-02	-2.77313E-02
$b_{18}$	0	-1.52212E-01	3.70714E-01
$b_{19}$	0	-5.58398E-04	1.16146E-03
$b_{20}$	0	1.30757E00	-2.23787E00
$b_{21}$	0	1.442206E02	1.292515E02
$b_{22}$	0	-2.544727E01	1.360552E00
$b_{23}$	0	-1.277055E02	-7.07482E01
$b_{24}$	0	2.236647E01	1.360532E00

<sup>a</sup> For  $Z \leq 0.25$ ,  $T = p(e, \rho)/\rho R$ .

Table A7. Coefficients for  $h = h(p, \rho)$  for  $-7.0 \leq Y \leq -4.5$

Coefficient	Values for range of $Z$ of ...					
	$Z \leq 0.10$	$0.10 < Z \leq 0.85$	$0.85 < Z \leq 1.30$	$1.30 < Z \leq 1.95$	$1.95 < Z$	
$c_1$	1.3986E00	2.53908E02	-1.05745E01	6.17584E-01	-8.32595E00	
$c_2$	0	1.01491E02	-1.93693E00	-2.40690E-01	-3.50219E-01	
$c_3$	0	-3.87199E02	3.07202E01	1.95904E00	1.36455E01	
$c_4$	0	-1.54304E02	3.35578E00	3.41644E-01	3.59350E-01	
$c_5$	0	7.28532E00	-7.79965E-02	-1.01073E-02	-3.70109E-03	
$c_6$	0	9.86233E01	-2.60637E01	-1.68951E00	-6.49007E00	
$c_7$	0	-8.04378E00	6.68790E-02	6.77631E-03	3.30836E-03	
$c_8$	0	4.63763E01	-1.42391E00	-1.10932E-01	-8.38594E-02	
$c_9$	0	-1.82577E-03	-9.86882E-04	-1.15922E-04	1.10018E-04	
$c_{10}$	0	2.18994E01	7.23223E00	4.26058E-01	1.02443E00	
$c_{11}$	0	-2.52423E02	-1.86342E01	-1.34222E01	-3.08441E01	
$c_{12}$	0	-1.01445E02	2.41997E-02	-5.43713E-01	-1.49510E00	
$c_{13}$	0	3.87210E02	3.20880E01	1.81528E01	3.00585E01	
$c_{14}$	0	1.54298E02	-7.46914E-01	3.95928E-01	9.19650E-01	
$c_{15}$	0	-7.2773E00	3.75161E-02	-7.41105E-03	-3.60024E-02	
$c_{16}$	0	-9.87576E01	-1.69985E01	-7.97425E00	-9.33522E00	
$c_{17}$	0	8.04277E00	-4.10125E-02	1.67768E-03	1.02522E-02	
$c_{18}$	0	-4.63883E01	5.39041E-01	-5.80593E-02	-1.35228E-01	
$c_{19}$	0	2.28399E-03	5.74637E-04	-3.32714E-06	-4.68760E-04	
$c_{20}$	0	-2.19438E01	2.56253E00	1.12448E00	8.92634E-01	
$c_{21}$	0	-11.0E00	2.768567E02	8.677803E01	8.800047E01	
$c_{22}$	0	2.0E00	2.152383E01	-8.370349E00	-1.679356E01	
$c_{23}$	0	11.0E00	-2.164837E02	-4.074084E01	-3.333353E01	
$c_{24}$	0	-2.0E00	-1.394837E01	7.407405E00	8.465574E00	
Sign	+	-	+	+	+	+

Table A8. Coefficients for  $h = h(p, \rho)$  for  $-4.5 < Y \leq -0.5$

Coefficient	Values for range of $Z$ of ----					
	$Z \leq 0.10$	$0.10 < Z \leq 0.95$	$0.95 < Z \leq 1.50$	$1.50 < Z \leq 2.00$	$2.00 < Z$	
c1	1.399E00	-1.33083E02	-7.36684E00	4.31520E-01	-3.77766E00	
c2	0	-9.98707E00	-1.13247E00	-2.83857E-01	-5.53738E-01	
c3	0	3.94734E02	2.47879E01	2.27791E00	6.60834E00	
c4	0	2.35810E01	1.99625E00	3.99159E-01	4.87181E-01	
c5	0	1.43957E00	-4.91630E-02	-1.29444E-02	-2.11045E-02	
c6	0	-3.84712E02	-2.3299E01	-1.84314E00	-2.94754E00	
c7	0	-1.43175E00	4.16673E-02	8.78724E-03	9.67277E-03	
c8	0	-1.36367E01	-8.59418E-01	-1.28136E-01	-1.02365E-01	
c9	0	1.77068E-05	-6.58149E-04	-1.60583E-04	-2.1942E-04	
c10	0	1.24325E02	7.19016E00	4.45362E-01	4.3962E-01	
c11	0	1.34486E02	-2.42647E00	-1.03883E01	4.05813E01	
c12	0	9.99122E00	5.57912E-01	-3.58718E-01	3.25692E00	
c13	0	-3.94719E02	-2.03055E00	1.35068E01	-4.79583E01	
c14	0	-2.35853E01	-1.22031E00	1.87268E-01	-2.53660E00	
c15	0	-1.43799E00	3.74866E-02	-4.28184E-03	9.06436E-02	
c16	0	3.84616E02	7.75414E00	-5.63894E00	1.8904E01	
c17	0	1.43039E00	-3.39278E-02	-9.52016E-04	-3.47578E-02	
c18	0	1.36318E01	6.08488E-01	-1.45625E-03	4.94114E-01	
c19	0	1.44367E-04	5.21012E-01	-4.10506E-05	1.00077E-03	
c20	0	-1.24348E02	-3.68326E00	7.39915E-01	-2.48554E00	
c21	0	-2.14144E01	8.077385E01	2.949221E02	5.34718E02	
c22	0	1.381584E00	-1.273807E01	1.36866E01	7.495657E01	
c23	0	2.039473E01	-6.547623E01	-1.559335E02	-2.219822E02	
c24	0	-1.315789E00	1.190475E01	-3.78776E00	-3.017229E01	
Sign	+	-	+	+	+	



Table A9. Coefficients for  $h = h(p, \rho)$  for  $-0.5 < Y \leq -3.0$

Coefficient	Values for range of $Z$ of			
	$Z \leq 0.10$	$0.10 < Z \leq 1.05$	$1.05 < Z \leq 1.60$	$1.60 < Z$
c1	1.4017E00	-9.67488E01	-2.67593E-01	9.21537E-01
c2	0	2.05296E-01	-1.87457E-01	-2.39670E-01
c3	0	2.69927E02	5.07693E00	1.30714E00
c4	0	-1.92887E00	2.72286E-01	3.4299E-01
c5	0	3.78392E-01	1.04541E-02	-2.18847E-02
c6	0	-2.46711E02	-5.0852E00	-1.20916E00
c7	0	-3.24965E-01	-1.42211E-02	1.36691E-02
c8	0	1.54416E00	-7.81935E-02	-1.10206E-01
c9	0	-3.61036E-03	6.38962E-04	-4.90274E-04
c10	0	7.48760E01	1.58711E00	3.087920E-01
c11	0	9.81502E01	2.87969E00	-6.77089E00
c12	0	-2.05448E-01	3.9009E-01	-6.90476E-02
c13	0	-2.69913E02	-8.06179E00	8.18168E00
c14	0	1.93052E00	-5.5125E-01	-9.52708E-02
c15	0	-3.78527E-01	-1.01903E-02	2.98487E-02
c16	0	2.46630E02	7.29592E00	-3.07662E00
c17	0	3.24832E-01	1.35906E-02	-1.78706E-02
c18	0	-1.54646E00	1.83861E-01	6.60408E-02
c19	0	3.66182E-03	-8.97772E-04	6.28419E-04
c20	0	-7.4898E01	-2.15153E00	3.38590E-01
c21	0	-2.659865E01	1.828573E02	1.5916669E02
c22	0	1.564631E00	-3.428596E01	3.976192E01
c23	0	2.312926E01	-1.51786E02	-7.966199E01
c24	0	-1.360543E00	2.976212E01	-1.66667E01
Sign	+	-	+	+

Table A10. Coefficients for  $T = T(p, \rho)$  for  $-7.0 \leq Y \leq -4.5$ 

Coefficient	Values <sup>a</sup> for range of $Z$ of --			
	$0.25 < Z \leq 0.95$	$0.95 < Z \leq 1.40$	$1.40 < Z \leq 1.95$	$1.95 < Z$
$d_1$	1.23718E-01	-8.12952E00	-1.98573E01	-2.33271E01
$d_2$	1.08623E-02	-8.28637E-01	-1.67225E00	-1.89958E00
$d_3$	2.24239E-01	2.26904E01	3.76159E01	3.21440E01
$d_4$	-8.24608E-02	1.41132E00	2.10964E00	1.68622E00
$d_5$	-1.17615E-03	-2.98633E-02	-3.40174E-02	-4.42123E-02
$d_6$	1.18397E00	-1.91806E01	-2.22215E01	-1.38645E01
$d_7$	-1.87566E-03	2.70066E-02	2.31712E-02	2.82629E-02
$d_8$	6.4852E-02	-5.78875E-01	-6.44596E-01	-3.40976E-01
$d_9$	-1.19155E-04	-2.28103E-04	-9.80275E-05	6.63272E-04
$d_{10}$	-5.52634E-01	5.62580E00	4.40486E00	2.04466E00
$d_{11}$	0	-3.99845E00	-5.36809E00	8.35474E00
$d_{12}$	0	2.26369E-01	2.41201E-01	1.71347E00
$d_{13}$	0	2.52870E00	-1.25881E00	-1.60715E01
$d_{14}$	0	-7.28448E-01	-8.62744E-01	-1.63139E00
$d_{15}$	0	1.09769E-02	-3.79774E-03	4.14641E-02
$d_{16}$	0	2.99238E00	5.58609E00	8.70275E00
$d_{17}$	0	-1.83819E-02	-7.81335E-03	-2.30068E-02
$d_{18}$	0	3.91440E-01	3.78963E-01	3.60966E-01
$d_{19}$	0	-1.51380E-04	-3.80005E-04	1.53246E-05
$d_{20}$	0	-2.04463E00	-1.81566E00	-1.46166E00
$d_{21}$	0	-3.887015E01	2.08E01	1.115884E02
$d_{22}$	0	-2.908228E01	-2.56E01	-6.452606E00
$d_{23}$	0	4.070557E01	1.0E00	-5.337863E01
$d_{24}$	0	2.682347E01	1.80E01	2.026986E00

<sup>a</sup>For  $Z \leq 0.25$ ,  $T = p/\rho R$ .

Table A11. Coefficients for  $T = T(p, \rho)$  for  $-4.5 < Y \leq -0.5$

Coefficient	Values <sup>a</sup> for range of $Z$ of -			
	$0.25 < Z \leq 0.95$	$0.95 < Z \leq 1.45$	$1.45 < Z \leq 2.05$	$2.05 < Z$
$d_1$	2.03910E-02	-5.12404E00	-1.23779E01	-1.27244E01
$d_2$	7.67310E-03	-2.8474E-01	-1.14728E00	-1.66684E00
$d_3$	8.48581E-01	1.54532E01	2.41382E01	1.72708E01
$d_4$	-2.93086E-02	4.52475E-01	1.38957E00	1.45307E00
$d_5$	8.40269E-04	-1.22881E-02	-3.63693E-02	-3.64515E-02
$d_6$	2.67251E-01	-1.35181E01	-1.42844E01	-6.97208E00
$d_7$	-1.47701E-03	8.56845E-03	2.24265E-02	1.90463E-02
$d_8$	2.37262E-02	-1.68725E-01	-4.06553E-01	-3.04323E-01
$d_9$	3.13687E-05	-3.25256E-04	-3.23888E-04	4.80787E-04
$d_{10}$	-1.41973E-01	4.18451E00	2.8762E00	9.67524E-01
$d_{11}$	0	7.52564E00	4.40782E00	7.71330E00
$d_{12}$	0	8.35238E-01	1.33046E00	5.0834E-01
$d_{13}$	0	-1.95558E01	-1.15405E01	-9.8211E00
$d_{14}$	0	-1.23393E00	-1.59892E00	-4.49138E-01
$d_{15}$	0	3.34510E-02	5.30580E-02	-9.41787E-04
$d_{16}$	0	1.71779E01	8.57309E00	4.16530E00
$d_{17}$	0	-2.34269E-02	-3.10376E-02	-2.40293E-03
$d_{18}$	0	4.54628E-01	4.71274E-01	9.63923E-02
$d_{19}$	0	4.81788E-04	4.77650E-04	-8.28450E-04
$d_{20}$	0	-5.09936E00	-1.96233E00	-5.88807E-01
$d_{21}$	0	6.148442E01	1.4075E02	-1.092654E03
$d_{22}$	0	-1.828123E01	-6.49992E00	-3.05312E02
$d_{23}$	0	-5.468755E01	-7.75E01	4.656243E02
$d_{24}$	0	1.562500E01	5.0E00	1.312498E02

<sup>a</sup>For  $Z \leq 0.25$ ,  $T = p/\rho R$ .

Table A12. Coefficients for  $T = T(p, \rho)$  for  $-0.5 < Y \leq -3.0$ 

Coefficient	Values <sup>a</sup> for range of $Z$ of —		
	$0.25 < Z \leq 1.00$	$1.00 < Z \leq 1.45$	$1.45 < Z$
$d_1$	-1.54141E-03	8.06492E-01	-1.66249E00
$d_2$	6.58337E-04	9.91293E-02	-8.91113E-02
$d_3$	9.82201E-01	-1.70742E00	4.11648E00
$d_4$	-3.85028E-03	-2.28264E-01	8.78093E-02
$d_5$	1.23111E-04	5.03500E-03	-3.09742E-03
$d_6$	3.77441E-02	3.02351E00	-1.84445E00
$d_7$	-4.08210E-04	-6.13927E-03	1.99879E-03
$d_8$	4.56963E-03	1.31574E-01	-7.50324E-03
$d_9$	2.13592E-05	1.69824E-04	6.85472E-05
$d_{10}$	-2.35172E-02	-1.12755E00	3.05784E-01
$d_{11}$	0	-1.17930E-01	1.11555E01
$d_{12}$	0	-2.12207E-01	1.3210E00
$d_{13}$	0	1.36524E00	-1.71236E01
$d_{14}$	0	4.05886E-01	-1.2919E00
$d_{15}$	0	-1.88260E-02	6.28124E-02
$d_{16}$	0	-2.10926E00	8.63804E00
$d_{17}$	0	1.65486E-02	-3.07949E-02
$d_{18}$	0	-1.89881E-01	3.07809E-01
$d_{19}$	0	-5.1140E-04	1.57743E-03
$d_{20}$	0	8.79806E-01	-1.42634E00
$d_{21}$	0	1.959604E02	1.330611E02
$d_{22}$	0	-4.269391E01	8.979635E00
$d_{23}$	0	-1.734931E02	-7.265298E01
$d_{24}$	0	3.762898E01	-2.449009E00

<sup>a</sup>For  $Z \leq 0.25$ ,  $T = p/\rho R$ .

Table A13. Coefficients for  $s = s(e, \rho)$

Coefficient	Values <sup>a</sup> for range of $Y$ of --		
	$-7.0 \leq Y \leq -4.5$	$-4.5 < Y \leq 0.5$	$0.5 < Y \leq 3.0$
$e_1$	-9.91081E-01	1.0836E01	2.01858E01
$e_2$	-5.00277E00	-4.55524E00	-3.13458E00
$e_3$	5.46521E01	2.96473E01	1.03619E01
$e_4$	5.10144E00	3.90851E00	1.87767E00
$e_5$	1.76206E-02	-2.05732E-03	-1.72922E-01
$e_6$	-2.97001E01	-1.67001E01	-5.43557E00
$e_7$	2.12002E-02	3.65982E-02	1.12174E-01
$e_8$	-1.84915E00	-1.44623E00	-8.71048E-01
$e_9$	1.76358E-03	5.23821E-03	1.28626E-02
$e_{10}$	5.87892E00	3.98307E00	2.01789E00

<sup>a</sup>For  $Z \leq 0.65$ ,  $s = 6779.2004 + |2.5(Z - 0.4) - Y|2.302585R$ .

Table A14. Coefficients for  $\rho = \rho(p, s)$

Coefficient	Values <sup>a</sup> for range of Y of --									
	1.23 ≤ Y < 1.42	1.42 ≤ Y < 1.592	1.592 ≤ Y < 1.70	1.70 ≤ Y < 1.80	1.80 ≤ Y < 1.90	1.90 ≤ Y < 2.00	2.00 ≤ Y ≤ 2.10	2.10 < Y		
$f_1$	-1.72119E01	-2.78074E02	1.10732E02	3.97149E01	6.22639E01	-2.99378E01	6.23124E02	1.40088E01	-3.62767E01	1.86938E02
$f_2$	5.49354E01	6.11791E02	-1.33968E02	-4.80988E01	-7.8884E01	3.89998E01	-6.77571E02	-1.58855E01	3.8634E01	-1.45261E02
$f_3$	-1.99776E00	1.37528E01	3.7583E-01	-1.17821E00	-2.19123E00	2.90256E00	9.12811E01	1.71245E-01	1.48507E00	2.23883E01
$f_4$	3.17884E00	-1.92394E01	2.77887E-01	1.27522E00	1.84533E00	-1.25088E00	-9.55480E01	4.32352E-01	-3.41824E-01	-1.04974E01
$f_5$	-4.69831E01	-4.42909E02	4.03018E01	1.45552E01	2.48413E01	-1.26684E01	1.84603E02	4.42836E00	-1.04718E01	2.60284E01
$f_6$	1.38567E-01	-1.97269E-01	1.18506E-01	-2.50279E-01	-8.76105E-02	6.13867E-02	6.97635E-01	-9.54417E-03	-3.25437E-02	1.85949E00
$f_7$	-8.66580E-01	7.10425E00	0	0	0	0	2.54274E01	0	0	0
$f_8$	-1.03055E-01	1.49708E-01	-6.98812E-02	1.58399E-01	5.55047E-02	-5.17059E-02	-3.27916E-01	8.92335E-03	1.22032E-02	-8.98218E-01
$f_9$	1.21069E01	1.05869E02	0	0	0	0	0	0	0	0
$f_{10}$	-1.52322E-03	1.19153E-03	0	0	0	0	4.90838E-03	0	0	0
$f_{11}$	0	2.80393E02	-6.85292E01	-5.01859E01	-7.28463E01	6.05677E01	-6.39514E02	-1.13217E02	6.5292E01	-1.27867E02
$f_{12}$	0	-5.95834E02	8.23834E01	6.31564E01	9.42375E01	-7.08307E01	6.97458E02	1.24304E02	-6.28154E01	8.58453E01
$f_{13}$	0	-1.75934E01	-1.24942E00	2.39925E00	4.04979E00	-2.95622E00	-1.00154E02	4.41505E00	2.10906E00	-2.28808E01
$f_{14}$	0	2.49706E01	8.31615E-01	-1.47883E00	-2.45467E00	1.70504E00	1.06701E02	-2.4853E00	-1.11759E00	1.13034E01
$f_{15}$	0	4.21767E02	-2.4524E01	-1.98852E01	-3.02865E01	2.07549E01	-1.90745E02	-3.42370E01	1.50026E01	-1.1234E01
$f_{16}$	0	3.61896E-01	-1.13019E-01	4.66791E-01	1.2872E-01	-2.70962E-01	-4.81471E-01	-7.84297E-02	2.71716E-01	-1.56005E00
$f_{17}$	0	-8.85461E00	0	0	0	0	-2.86323E01	0	0	0
$f_{18}$	0	-2.55458E-01	7.46719E-02	3.06926E-01	-8.63721E-02	1.80057E-01	2.00348E-01	1.21459E-02	-1.4431E-01	7.79397E-01
$f_{19}$	0	-9.94515E01	0	0	0	0	0	0	0	0
$f_{20}$	0	-2.96892E-03	0	0	0	0	-6.43371E-03	0	0	0
$f_{21}$	0	-8.12685E02	9.9318E01	3.6406E01	3.672E01	5.8278E01	1.17248E02	7.308E01	2.65925E02	5.2614E01
$f_{22}$	0	1.304205E03	-6.7952E01	-2.232E01	2.69152E01	-3.3644E01	-7.055E01	-4.1768E01	-1.4142E02	-3.0086E01
$f_{23}$	0	0	-2.0E00	-2.0E00	-2.0E00	-2.0E00	-2.0E00	-2.0E00	-5.0E00	-2.0E00
$f_{24}$	0	-1.5E01	0	0	0	0	0	0	0	0
$f_{25}$	0	-5.03745E02	0	0	0	0	0	0	0	0

<sup>a</sup> For  $Y < 1.23$ ,  $\ln(\rho/p_0) = [\ln(\rho/p_0)/1.40] - (s - s_0)/3.5R$ .

Table A15. Coefficients for  $\epsilon = \epsilon(p, s)$

Coefficient	Values <sup>a</sup> for range of $Y$ of —									
	$1.23 \leq Y \leq 1.40$	$1.40 < Y < 1.592$	$1.592 \leq Y < 1.70$ ( $Z > -1.917E00Y$ + 0.092E00)	$1.70 \leq Y < 1.80$ ( $Z \leq -1.917E00Y$ + 0.092E00)	$1.70 \leq Y < 1.80$ ( $Z > -1.917E00Y$ + 0.092E00)	$1.80 \leq Y < 1.90$	$1.90 \leq Y < 2.00$	$2.00 \leq Y < 2.10$	$2.10 \leq Y$	
91	4.89511E01	1.30563E02	3.39933E01	-1.66572E01	1.94882E01	-6.37715E01	-1.75434E01	-1.18487E01	-2.40636E01	
92	-1.15989E02	-2.87254E02	4.02792E01	1.51243E01	2.31472E01	5.46005E01	2.00307E01	1.26558E01	3.35589E00	
93	-4.43026E-01	-7.71873E00	7.62742E-01	-4.72897E-01	1.00783E00	-8.90073E00	6.20484E-01	6.09885E-04	-1.14521E01	
94	1.49819E00	1.17605E01	-3.79044E-01	2.95848E-01	-5.18103E-01	5.02063E00	-2.76756E-01	5.90396E-02	5.62572E00	
95	8.70709E01	2.06757E02	-1.09895E01	-2.31418E00	-5.92829E00	-9.67094E00	-4.76084E00	-2.45275E00	4.93842E00	
96	-5.08747E-02	1.64299E-01	-7.13412E-02	-3.61191E-02	9.92242E-02	-7.13493E-01	1.14921E-02	-6.70888E-03	-7.55608E-01	
97	-7.02417E-01	-4.31838E00	0	0	0	0	0	0	0	
98	2.94929E-02	-1.21768E-01	4.22359E-02	1.7288E-02	-5.67928E-02	3.97962E-01	-5.80043E-03	5.21033E-03	3.69774E-01	
99	-2.04916E01	-4.83472E01	0	0	0	0	0	0	0	
910	5.24685E-04	-1.26118E-03	0	0	0	0	0	0	0	
911	0	-8.4598E01	3.32182E01	-3.27168E00	-2.09813E00	5.05131E01	1.10485E01	3.39157E00	2.23905E01	
912	0	1.74701E02	-4.03847E01	9.45383E00	1.22781E00	-3.97363E01	-1.261E01	-3.835E00	-1.90842E00	
913	0	9.52234E00	1.87601E-01	2.04E00	-6.27531E-01	9.27248E00	-6.59043E-01	-2.14031E-01	1.05618E01	
914	0	-1.32819E01	-1.07599E-01	-1.1342E00	3.71651E-01	-5.15576E00	3.66266E-01	9.90508E-02	-5.17247E00	
915	0	-1.20234E02	1.22657E01	-4.28765E00	9.84125E-04	6.45632E00	3.59417E00	1.07008E00	-4.3714E00	
916	0	-2.27725E-01	-1.65537E-01	1.5021E-01	-1.24024E-01	7.2563E-01	-6.04061E-03	-7.87516E-02	6.27818E-01	
917	0	4.6271E00	0	0	0	0	0	0	0	
918	0	1.60365E-01	1.02560E-01	-8.27388E-02	7.65034E-02	-4.03054E-01	6.78382E-03	3.63642E-02	-3.12015E-01	
919	0	2.75818E01	0	0	0	0	0	0	0	
920	0	1.4933E-03	0	0	0	0	0	0	0	
921	0	-8.12685E02	4.8092E01	4.6708E01	6.2192E01	1.17248E02	7.308E01	2.65925E02	5.2614E01	
922	0	1.304205E03	-2.8124E01	-3.399E01	-3.6304E01	-7.055E01	-4.1768E01	-1.4142E02	-3.0096E01	
923	0	0	-2.0E00	-2.0E00	-2.0E00	-2.0E00	-2.0E00	-5.0E00	-2.0E00	
924	0	-1.5E01	0	0	0	0	0	0	0	
925	0	-5.03745E02	0	0	0	0	0	0	0	

<sup>a</sup> For  $Y < 1.23$ ,  $\ln(\epsilon/2.5\epsilon_0) = [\ln(p/p_0) + (s - s_0)R]/3.5$ .

Table A16. Coefficients for  $\alpha = \alpha(p, s)$ 

Coefficient	Values <sup>a</sup> for range of Y of --									
	$1.23 < Y \leq 1.40$	$1.40 < Y < 1.595$	$1.595 \leq Y < 1.693$ ( $Z \leq -9.842Y$ + 14.19)	$1.693 \leq Y < 1.693$ ( $Z > -9.842Y$ + 14.19)	$1.693 \leq Y < 1.80$ ( $Z \leq -1.917Y$ + 0.092)	$1.693 \leq Y < 1.80$ ( $Z > -1.917Y$ + 0.092)	$1.80 \leq Y < 1.90$	$1.90 \leq Y < 2.00$	$2.00 \leq Y < 2.10$	$2.10 \leq Y$
$h_1$	-1.38377E-01	1.31057E02	-6.13548E01	3.37056E00	-8.04927E01	-4.73308E00	-6.60574E02	-5.93354E00	7.02453E01	1.12793E02
$h_2$	-8.84138E00	-2.88847E02	7.80742E01	-4.87016E00	7.63739E01	4.69363E00	7.38042E02	-7.79929E00	-7.34732E01	1.35296E02
$h_3$	2.61050E00	-5.04887E00	2.08524E00	-3.85754E-01	-9.381E00	9.43798E-02	-8.77589E01	-7.23618E00	5.86844E-01	2.74295E00
$h_4$	3.16535E00	7.73862E00	-1.21609E00	2.87192E-01	5.72104E00	3.54953E-03	9.7894E01	3.31162E00	0	0
$h_5$	1.10866E01	2.10147E02	-2.43686E01	2.02041E00	-1.63435E01	-7.98293E-01	-2.06156E02	5.06381E00	1.95548E01	-4.08171E01
$h_6$	-1.00224E-01	5.48031E-02	8.77563E-02	-4.63144E-03	7.48578E-01	2.02561E-02	-2.14028E-02	-5.37773E-01	7.36786E-03	-2.25652E-01
$h_7$	9.88389E-01	-2.88963E00	0	0	0	0	-2.73753E01	0	1.81521E-01	-1.29257E00
$h_8$	6.62193E-02	-4.39459E-02	-5.46311E-02	8.30832E-03	4.50043E-01	-8.73036E-03	0	2.46865E-01	0	0
$h_9$	-3.25761E00	-5.0396E01	0	0	0	0	0	0	0	0
$h_{10}$	8.20610E-04	-2.10202E-04	0	0	0	0	0	0	0	0
$h_{11}$	0	-1.33465E02	2.07952E01	0	8.34054E01	0	6.65014E02	3.9526E01	-1.6961E01	2.57057E02
$h_{12}$	0	2.84739E02	-2.71591E01	0	-8.58837E01	0	-7.43416E02	-2.90994E01	1.80169E01	-2.83199E02
$h_{13}$	0	7.57389E00	-7.43673E-01	0	4.84197E00	0	8.87679E01	6.24136E00	-3.65779E-01	-5.84656E00
$h_{14}$	0	-1.07749E01	4.08312E-01	0	-3.11188E00	0	-9.90508E01	-2.70007E00	0	0
$h_{15}$	0	-2.02362E02	8.68124E00	0	2.11196E01	0	2.08117E02	5.42786E00	-4.75063E00	7.91574E01
$h_{16}$	0	1.53453E-01	-9.3592E-02	0	2.33945E-01	0	2.81148E-02	5.95235E-01	2.01803E-02	3.35638E-01
$h_{17}$	0	3.8313E00	0	0	0	0	2.77374E01	0	1.07583E-01	2.17312E00
$h_{18}$	0	1.08531E-01	5.32328E-02	0	-1.59099E-01	0	0	-2.67771E-01	0	0
$h_{19}$	0	4.79075E01	0	0	0	0	0	0	0	0
$h_{20}$	0	9.7931E-04	0	0	0	0	0	0	0	0
$h_{21}$	0	8.12685E02	1.14314E02	0	1.5138E01	0	1.17248E02	4.03352E01	2.65925E02	5.2614E01
$h_{22}$	0	1.304205E03	-7.757E01	0	-1.5748E01	0	7.055E01	-2.73502E01	-1.4142E02	-3.0096E01
$h_{23}$	0	0	-2.0E00	0	-2.0E00	0	-2.0E00	-2.0E00	-5.0E00	-2.0E00
$h_{24}$	0	-1.5E01	0	0	0	0	0	0	0	0
$h_{25}$	0	-5.03745E02	0	0	0	0	0	0	0	0

<sup>a</sup> For  $Y < 1.23$ ,  $\ln \alpha^2 = \ln(1.4p_0/\rho_0) + |\ln(p/p_0) + (s - s_0)/R|/3.5$ .



## Appendix B

### Master Program

All the curve fits developed in this study have been incorporated into a single master program called TGAS. This master program permits the user to select the desired curve fit from a menu of possibilities. The calling statement for this subroutine is

```
CALL TGAS (P,RHO,E,H,T,A,S,NTGAS)
```

where

P	pressure, N/m <sup>2</sup>
RHO	density, kg/m <sup>3</sup>
E	specific internal energy, m <sup>2</sup> /s <sup>2</sup>
H	specific enthalpy, m <sup>2</sup> /s <sup>2</sup>
T	temperature, K
A	speed of sound, m/s
S	specific entropy, m <sup>2</sup> /s <sup>2</sup> -K
NTGAS	integer flag to be set by the user for selection of the appropriate curve fit as follows:

NTGAS = 0:	$p = p(e, \rho)$
NTGAS = 1:	$p = p(e, \rho),$ $a = a(e, \rho)$
NTGAS = 2:	$p = p(e, \rho),$ $T = T(e, \rho)$
NTGAS = 3:	$p = p(e, \rho),$ $a = a(e, \rho),$ $T = T(e, \rho)$
NTGAS = 4:	$s = s(e, \rho)$
NTGAS = 5:	$T = T(p, \rho)$
NTGAS = 6:	$h = h(p, \rho)$
NTGAS = 7:	$\rho = \rho(p, s)$
NTGAS = 8:	$e = e(p, s)$
NTGAS = 9:	$a = a(p, s)$

The curve fits for  $p = p(e, \rho)$ ,  $a = a(e, \rho)$ , and  $T = T(e, \rho)$  have been placed in the single subroutine TGAS1. Subroutine TGAS2 computes  $s = s(e, \rho)$ , subroutine TGAS3 computes  $T = T(p, \rho)$ , and subroutine TGAS4 computes  $h = h(p, \rho)$ . The curve fits for  $\rho = \rho(p, s)$ ,  $e = e(p, s)$ , and  $a = a(p, s)$  have been placed in subroutines TGAS5, TGAS6, and TGAS7, respectively. The subroutines TGAS1 to TGAS7 can be used in a "stand-alone" manner if so desired, independent of the master program. A FORTRAN listing of each subroutine is given in reference 18.

## References

1. Gilmore, F. R.: *Equilibrium Composition and Thermodynamic Properties of Air to 24,000° K.* U.S. Air Force Proj. Rand Res. Memo. RM-1543, Rand Corp., Aug. 24, 1955. (Available from DTIC as AD 840 52.)
2. Hilsenrath, Joseph; and Beckett, Charles W.: *Tables of Thermodynamic Properties of Argon-Free Air to 15,000° K.* AEDC-TN-56-12, Arnold Engineering Development Center, Sept. 1956. (Available from DTIC as AD 989 74.)
3. Hansen, C. Frederick: *Approximations for the Thermodynamic and Transport Properties of High-Temperature Air.* NASA TR R-50, 1959. (Supersedes NACA TN 4150.)
4. Moeckel, W. E.; and Weston, Kenneth C.: *Composition and Thermodynamic Properties of Air in Chemical Equilibrium.* NACA TN 4265, 1958.
5. Bailey, Harry E.: *Programs for Computing Equilibrium Thermodynamic Properties of Gases.* NASA TN D-3921, 1967.
6. Zeleznik, Frank J.; and Gordon, Sanford: *A General IBM 704 or 7090 Computer Program for Computation of Chemical Equilibrium Compositions, Rocket Performance, and Chapman-Jouguet Detonations.* NASA TN D-1454, 1962.
7. Gordon, Sanford; and McBride, Bonnie J.: *Computer Program for Calculation of Complex Chemical Equilibrium Compositions, Rocket Performance, Incident and Reflected Shocks, and Chapman-Jouguet Detonations.* NASA SP-273, 1971.
8. Miner, E. W.; Anderson, E. C.; and Lewis, Clark H.: *A Computer Program for Two-Dimensional and Axisymmetric Nonreacting Perfect Gas and Equilibrium Chemically Reacting Laminar, Transitional and-or Turbulent Boundary Layer Flows.* VPI-E-71-8 (Contract NAS1-9337), Dep. Aerospace Engineering, Virginia Polytechnic Inst., Jan. 1975. (Available as NASA CR-132601.)
9. Lomax, Harvard; and Inouye, Mamoru: *Numerical Analysis of Flow Properties About Blunt Bodies Moving at Supersonic Speeds in an Equilibrium Gas.* NASA TR R-204, 1964.
10. Tannehill, J. C.; and Mohling, R. A.: *Development of Equilibrium Air Computer Programs Suitable for Numerical Computation Using Time-Dependent or Shock-Capturing Methods.* NASA CR-2134, 1972.
11. Grabau, Martin: *A Method of Forming Continuous Empirical Equations for the Thermodynamic Properties of Air From Ambient Temperatures to 15,000° K, With Applications.* AEDC-TN-59-102 (Contract No. AF 40 (600)-800), Arnold Engineering Development Center, Aug. 1959.
12. Lewis, Clark H.; and Burgess, Ernest G., III: *Empirical Equations for the Thermodynamic Properties of Air and Nitrogen to 15,000° K.* AEDC-TDR-63-138, U.S. Air Force, July 1963.
13. Barnwell, Richard W.: *Inviscid Radiating Shock Layers About Spheres Traveling at Hyperbolic Speeds in Air.* NASA TR R-311, 1969.
14. Viegas, John R.; and Howe, John T.: *Thermodynamic and Transport Property Correlation Formulas for Equilibrium Air From 1,000° K to 15,000° K.* NASA TN D-1429, 1962.
15. Tannehill, J. C.; and Mugge, P. H.: *Improved Curve Fits for the Thermodynamic Properties of Equilibrium Air Suitable for Numerical Computation Using Time-Dependent or Shock-Capturing Methods.* NASA CR-2470, 1974.
16. Vigneron, Yvon Clovis: *Hypersonic Viscous Flow of Equilibrium Air Around a Blunt Body.* M.S. Thesis, Iowa State Univ., 1976.
17. Hemmerle, William J.: *Statistical Computations on a Digital Computer.* Blaisdell Publ. Co., c.1967.
18. Srinivasan, S.; Tannehill, J. C.; and Weilmuenster, K. J.: *Simplified Curve Fits for the Thermodynamic Properties of Equilibrium Air.* ISU-ERI-Ames-86401 (Grant NAG-1-313), Engineering Research Inst., Iowa State Univ., June 1986.









# Report Documentation Page

1. Report No. NASA RP-1181		2. Government Accession No.		3. Recipient's Catalog No.	
4. Title and Subtitle Simplified Curve Fits for the Thermodynamic Properties of Equilibrium Air				5. Report Date August 1987	
				6. Performing Organization Code	
7. Author(s) S. Srinivasan, J. C. Tannehill, and K. J. Weilmuenster				8. Performing Organization Report No. L-16276	
9. Performing Organization Name and Address Langley Research Center Hampton, Virginia 23665-5225				10. Work Unit No. 506-51-13-03	
				11. Contract or Grant No.	
12. Sponsoring Agency Name and Address National Aeronautics and Space Administration Washington, DC 20546-0001				13. Type of Report and Period Covered Reference Publication	
				14. Sponsoring Agency Code	
15. Supplementary Notes S. Srinivasan and J. C. Tannehill: Iowa State University, Ames, Iowa. K. J. Weilmuenster: Langley Research Center, Hampton, Virginia. This work was supported by NASA Langley Research Center under Grant NAG-1-313.					
16. Abstract New, improved curve fits for the thermodynamic properties of equilibrium air have been developed. The curve fits are for pressure, speed of sound, temperature, entropy, enthalpy, density, and internal energy. These curve fits can be readily incorporated into new or existing computational fluid dynamics codes if "real-gas" effects are desired. The curve fits are constructed from Grabau-type transition functions to model the thermodynamic surfaces in a piecewise manner. The accuracies and continuity of these curve fits are substantially improved over those of previous curve fits. These improvements are due to the incorporation of a small number of additional terms in the approximating polynomials and careful choices of the transition functions. The ranges of validity of the new curve fits are temperatures up to 25000 K and densities from $10^{-7}$ to $10^3$ amagats.					
17. Key Words (Suggested by Authors(s)) Equilibrium air Curve fits Computational fluid dynamics Hypersonic flow			18. Distribution Statement Unclassified Unlimited  Subject Category 34		
19. Security Classif.(of this report) Unclassified		20. Security Classif.(of this page) Unclassified		21. No. of Pages 47	22. Price A03